JLAB-THY-10-1160

High-energy amplitudes in the next-to-leading order

Ian Balitsky
Physics Dept., ODU, Norfolk VA 23529,
and
Theory Group, Jlab, 12000 Jefferson Ave,
Newport News, VA 23606 *
(Dated: April 2, 2010)

I review the calculation of the next-to-leading order behavior of high-energy amplitudes in $\mathcal{N}=4$ SYM and QCD using the operator expansion in Wilson lines.

PACS numbers: 12.38.Bx, 12.38.Cy

Contents

I. INTRODUCTION

The standard way to analyze the high-energy behavior of pQCD amplitudes is the direct summation of Feynman diagrams. In the Regge limit $s >> t, m^2$ (where m is a characteristic mass or virtuality of colliding particles) there is an extra parameter in addition to α_s, namely $\alpha_s \ln\frac{s}{m^2}$. At pre-asymptotic energies we may have a window where the leading logarithmic approximation (LLA)

$$\alpha_s \ll 1, \qquad \alpha_s \ln\frac{s}{m^2} \sim 1 \tag{1}$$

*Electronic address: balitsky@jlab.org

is valid. Following the pioneering work by Lipatov [1], the amplitude in this region of energies was shown to be determined by the BFKL pomeron [2] which leads to the behavior of QCD cross sections of the type

$$\sigma(s) \;=\; \int d\nu\, \Big(\frac{s}{m^2}\Big)^{\omega(\nu)} F(\nu) \;\sim\; \Big(\frac{s}{m^2}\Big)^{4\frac{\alpha_s}{\pi}N_c\ln 2} \tag{2}$$

where N_c is a number of colors ($N_c = 3$ for QCD), $\omega(\nu) = \frac{\alpha_s}{\pi}N_c[2\psi(1) - \psi(\frac{1}{2}+i\nu) - \psi(\frac{1}{2}-i\nu)]$ is the BFKL intercept, and $F(\nu)$ is the "pomeron residue" which depends on the process.

The power behavior of the cross section (2) violates the Froissart bound $\sigma \leq \ln^2 s$, and therefore the BFKL pomeron describes only the pre-asymptotic behavior at intermediate energies when the cross sections are small in comparison to the geometric cross section $2\pi R^2$. In order to find the exact window of the BFKL applicability one needs to calculate the first correction to the BFKL amplitude.

The importance of corrections to LLA result in high-energy QCD is twofold. As I mentioned above, to get the region of application of a leading-order result one needs to find the next-to-leading order (NLO) corrections. However, in the case of the BFKL amplitude (2) there is another reason why NLO corrections are essential. Unlike for example the DGLAP evolution, the argument of the coupling constant in Eq. (2) is left undetermined in the LLA, and usually it is set by hand to be of order of characteristic transverse momenta. Careful analysis of this argument is very important from both theoretical and experimental points of view, and the starting point of the analysis of the argument of α_s in Eq. (2) is the calculation of the NLO BFKL correction.

The NLO correction to the BFKL pomeron intercept $\omega(\nu)$ was found by two groups - Lipatov and Fadin [3] and Ciafaloni and Camichi [4] - after almost ten years of calculations. The result has the form

$$\begin{aligned}\omega(\nu) \;&=\; \frac{\alpha_s}{\pi}N_c\Big[\chi(\nu) + \frac{\alpha_s N_c}{4\pi}\delta(\nu)\Big],\\ \delta(\nu) \;&=\; -\frac{b}{2N_c}\chi^2(\nu) + 6\zeta(3) + \Big[\frac{67}{9} - \frac{\pi^2}{3} - \frac{10n_f}{9N_c}\Big]\chi(\nu) + \chi''(\nu) - \; 2\Phi(\nu) - 2\Phi(-\nu)\end{aligned} \tag{3}$$

where $b = \frac{11}{3}N_c - \frac{2}{3}n_f$, $\chi(\nu) = -2C - \psi(\frac{1}{2}+i\nu) - \psi(\frac{1}{2}-i\nu)$ ($C = -\psi(1)$ is Euler's constant), and

$$\Phi(\nu) \;=\; -\int_0^1 \frac{dt}{1+t}\, t^{-\frac{1}{2}+i\nu}\Big[\frac{\pi^2}{6} + 2\mathrm{Li}_2(t)\Big]. \tag{4}$$

The term proportional to b depends on the choice of the argument of coupling constant. The choice of this term in the r.h.s. of Eq. (3) corresponds to $\alpha(q_1q_2)$ where q_i are momenta of scattered BFKL gluons, see the discussion in Ref. [3]. The pomeron intercept is related to anomalous dimensions of the twist-2 gluon operators - it determines the asymptotics of anomalous dimensions γ_j as $j-1=\omega\to 0$. It is worth noting that the result of explicit calculation of 3-loop anomalous dimensions at the 3-loop level [5] agrees with Eq. (3). As we see from Eq. (3) the full NLO description of the amplitude implies the knowledge of the "pomeron residue" $F(\nu)$ at the NLO level. A classical example is the scattering of virtual photons in QCD where $F(\nu)$ is proportional to product of two amplitudes of emission of two t-channel gluons by the upper and the lower virtual photon. In the leading order, these "impact factors" are known for a long time since they differ from the corresponding QED result only by trivial color factors. However, to the best of my knowledge, there is no complete analytical calculation of the NLO photon impact factor in the literature (for a combination of numerical and analytical results, see Ref. [6]). I will present the analytical result for the photon impact factor in the coordinate space which is compact and conformally invariant; however, the Fourier transformation to the momentum space is not performed yet. The calculations use different approach to high-energy scattering based on the operator expansion in Wilson lines [7] rather than on the direct summation of Feynman diagrams.

A general feature of high-energy scattering is that a fast particle moves along its straight-line classical trajectory and the only quantum effect is the eikonal phase factor acquired along this propagation path. In QCD, for the fast quark or gluon scattering off some target, this eikonal phase factor is a Wilson line - the infinite gauge link ordered along the straight line collinear to particle's velocity n^μ:

$$U^Y(x_\perp) = \mathrm{Pexp}\Big\{-ig\int_{-\infty}^{\infty} du\; n_\mu\; A^\mu(un + x_\perp)\Big\}, \tag{5}$$

Here A_μ is the gluon field of the target, $x_\perp$ is the transverse position of the particle which remains unchanged throughout the collision, and the index Y labels the rapidity of the particle. Repeating the above argument for the target (moving fast in the spectator's frame) we see that particles with very different rapidities perceive each other as Wilson lines and therefore these Wilson-line operators form the convenient effective degrees of freedom in high-energy QCD (for a review, see ref. [8]).

As an example of high-energy process let us consider the deep inelastic scattering from a hadron at small $x_B = Q^2/(2p\cdot q)$. The virtual photon decomposes into a pair of fast quarks moving along straight lines separated by some transverse distance. The propagation of this quark-antiquark pair reduces to the "propagator of the color dipole" $U(x_\perp)U^\dagger(y_\perp)$ - two Wilson lines ordered along the direction collinear to quarks' velocity. The structure function of a hadron is proportional to a matrix element of this color dipole operator

$$\hat{\mathcal{U}}^Y(x_\perp,y_\perp) = 1 - \frac{1}{N_c}\mathrm{Tr}\{\hat{U}^Y(x_\perp)\hat{U}^{\dagger Y}(y_\perp)\} \tag{6}$$

switched between the target's states ($N_c = 3$ for QCD). The gluon parton density is approximately

$$x_B G(x_B,\mu^2 = Q^2) \ \simeq \ \langle p|\,\hat{\mathcal{U}}^Y(x_\perp,0)|p\rangle\Big|_{x_\perp^2=Q^{-2}} \tag{7}$$

where $Y = \ln\frac{1}{x_B}$. (As usual, we denote operators by "hat"). The energy dependence of the structure function is translated then into the dependence of the color dipole on on the rapidity Y. There are two ways to restrict the rapidity of Wilson lines: one can consider Wilson lines with the support line collinear to the velocity of the fast-moving particle or one can take the light-like Wilson line and cut the rapidity integrals "by hand" (see Eq. (30) below). While the former method appears to be more natural, it is technically simpler to get the final results with the latter method of "rigid cutoff" in the longitudinal direction.

Eq. (7) means that the small-x behavior of the structure functions is governed by the rapidity evolution of color dipoles [9, 10]. At relatively high energies and for sufficiently small dipoles we can use the leading logarithmic approximation (1) ($\alpha_s \ll 1,\ \alpha_s\ln x_B \sim 1$) and get the non-linear BK evolution equation for the color dipoles [7, 11]:

$$\frac{d}{dY}\,\hat{\mathcal{U}}^Y(z_1,z_2) \ = \ \frac{\alpha_s N_c}{2\pi^2}\int d^2z_3\ \frac{z_{12}^2}{z_{13}^2z_{23}^2}[\hat{\mathcal{U}}^Y(z_1,z_3) + \hat{\mathcal{U}}^Y(z_3,z_2)) - \hat{\mathcal{U}}^Y(z_1,z_3) - \hat{\mathcal{U}}^Y(z_1,z_3)\hat{\mathcal{U}}^Y(z_3,z_2)] \tag{8}$$

where $Y = \ln\frac{1}{x_B}$ and $z_{12} \equiv z_1 - z_2$ etc. The first three terms correspond to the linear BFKL evolution [2] and describe the parton emission while the last term is responsible for the parton annihilation. For sufficiently low x_B the parton emission balances the parton annihilation so the partons reach the state of saturation [12] with the characteristic transverse momentum Q_s growing with energy $1/x_B$ (for reviews, see Ref. [13])

It is easy to see that the BK equation (8) is conformally invariant in the two-dimensional space. This follows from the conformal invariance of the light-like Wilson lines. The Wilson line

$$U(x_\perp) \ = \ \mathrm{Pexp}\Big\{-ig\int_{-\infty}^{\infty}dx^+\ A_+(x^+,x_\perp)\Big\} \tag{9}$$

is invariant under the inversion $x^\mu \to x^\mu/x^2$ (with respect to the point with zero (-) component). Indeed, $(x^+,x_\perp)^2 = x_\perp^2$ so after the inversion $x_\perp \to x_\perp/x_\perp^2$ and $x^+ \to x^+/x_\perp^2$ and therefore

$$U(x_\perp) \ \to \ \mathrm{Pexp}\Big\{-ig\int_{-\infty}^{\infty}d\frac{x^+}{x_\perp^2}\ A_+(\frac{x^+}{x_\perp^2},x_\perp)\Big\} \ = \ U(x_\perp/x_\perp^2) \tag{10}$$

Moreover, it is easy to check formally that the Wilson line operators lie in the standard representation of the conformal Möbius group SL(2,C) with conformal spin 0 (see [14])). It should be noted that the conformal invariance of the linear BFKL equation was first proved in Ref. [15].

The NLO evolution of color dipole in QCD is not expected to be Möbius invariant due to the conformal anomaly leading to dimensional transmutation and running coupling constant. To understand the relation between the high-energy behavior of amplitudes and Möbius invariance of Wilson lines, it is instructive to consider the conformally invariant $\mathcal{N} = 4$ super Yang-Mils theory. This theory was intensively studied in recent years due to the fact that at large coupling constants it is dual to the IIB string theory in the AdS$_5$ background. In the light-cone limit, the contribution of scalar operators to Maldacena-Wilson line [16] vanishes so one has the usual Wilson line constructed from gauge fields and therefore the LLA evolution equation for color dipoles in the $\mathcal{N} = 4$ SYM has the same form as (8). At the NLO level, the contributions from gluino and scalar loops enter the game.

As I mentioned above, formally the light-like Wilson lines are Möbius invariant. However, the light-like Wilson lines are divergent in the longitudinal direction and moreover, it is exactly the evolution equation with respect to this longitudinal cutoff which governs the high-energy behavior of amplitudes. At present, it is not known how to find the conformally invariant cutoff in the longitudinal direction. When we use the non-invariant cutoff we expect, as usual, the invariance to hold in the leading order but to be violated in higher orders in perturbation theory. In our calculation we restrict the longitudinal momentum of the gluons composing Wilson lines, and with this non-invariant

cutoff the NLO evolution equation in QCD has extra non-conformal parts not related to the running of coupling constant. Similarly, there will be non-conformal parts coming from the longitudinal cutoff of Wilson lines in the $\mathcal{N}=4$ SYM equation. I will demonstrate below that it is possible to construct the "composite conformal dipole operator" (order by order in perturbation theory) which mimics the conformal cutoff in the longitudinal direction so the corresponding evolution equation is Möbius invariant. With the NLO accuracy this composite operator has the form [14] (a is an arbitrary constant):

$$[\mathrm{Tr}\{\hat{U}_{z_1}\hat{U}^\dagger_{z_2}\}]^{\rm conf}_{a,Y} \tag{11}$$
$$= \ \mathrm{Tr}\{\hat{U}^\sigma_{z_1}\hat{U}^{\dagger\sigma}_{z_2}\} + \frac{\alpha_s}{2\pi^2}\int d^2z_3\ \frac{z_{12}^2}{z_{13}^2 z_{23}^2}[\mathrm{Tr}\{T^n\hat{U}^\sigma_{z_1}\hat{U}^{\dagger\sigma}_{z_3}T^n\hat{U}^\sigma_{z_3}\hat{U}^{\dagger\sigma}_{z_2}\} - N_c\mathrm{Tr}\{\hat{U}^\sigma_{z_1}\hat{U}^{\dagger\sigma}_{z_2}\}]\ln\frac{4az_{12}^2}{sz_{13}^2 z_{23}^2}\ +\ O(\alpha_s^2)$$

where the second term is a "counterterm" restoring the conformal invariance lost because of the cutoff (30). This is quite similar to the construction of the composite renormalized local operator in the case when the UV cutoff does not respect the symmetries of the bare operator - in this case the symmetry of the UV-regularized operator is preserved order by order in perturbation theory by subtraction of the symmetry-restoring counterterms.

The NLO BK equation written in terms of these composite conformal operators is conformally invariant (in $\mathcal{N}=4$ SYM) and so are the impact factors [14]. Below I present the results for these impact factors and for the "pomeron residue" $F(\nu)$ in a simple case of correlator of four scalar currents in the Regge limit.

In QCD we do not have the conformal invariance so the corresponding composite operators are not, strictly speaking, conformal. Still, if we write down the NLO BK equation in terms of these operators it has a nice property of being a sum of conformal part and the running-coupling part proportional to $b=\frac{11}{3}N_c-\frac{2}{3}n_f$. I calculate the NLO coefficient function in the expansion of two electromagnetic currents in these composite operators which determines the photon impact factor at the NLO level.

The paper is organized as follows. In Sect. II I remind the general logic of the operator expansion using the example of light-ray OPE. In Sect. III I formulate the program of high-energy OPE and carry it out in subsequent Sections. In Sect IV we calculate the high-energy amplitudes in $\mathcal{N}=4$ SYM in the leading order and then in the NLO. Sect V is devoted to the NLO high-energy amplitudes in QCD and Sect. VI contains the conclusions. The details of the calculation of Feynman diagrams for the NLO evolution of color dipoles are not presented here (see the original publications [14, 17–19]) but we will outline the calculation of impact factors in $\mathcal{N}=4$ SYM and in QCD.

II. THE LOGIC OF OPE

Let me first remind the logic of usual operator expansion near the light cone. A typical example is the calculation of the structure functions of deep inelastic scattering (DIS) at moderate $x_B=Q^2/(2p\cdot q)$ determined by the T-product of two electromagnetic currents $T\{j_\mu(x)j_\nu(y)\}$ switched between the target states. The first step is to identify the relevant operators. To this end, we formally put Q^2 to infinity, then $(x-y)^2=0$ and we see that the relevant operators are the light-ray ones of the type of $\bar\psi(x)\gamma_\mu[x,y]\psi(y)$ where

$$[x,y]\ \equiv\ \mathrm{Pexp}\Big\{-ig\int_0^1du\ (x-y)^\mu A_\mu(ux-uy+y)\Big\} \tag{12}$$

is a standard notation for a straight-line gauge link connecting points x and y.

Now, to get the Q^2 behavior of structure functions one needs to perform the following four steps:

- Separate relevant Feynman loop integrals over $k_\perp$ in two parts - the coefficient functions (with transverse momenta $k_\perp^2$ greater than the factorization scale μ^2) and parton densities - matrix elements of light-ray operators with $k_\perp^2<\mu^2$ (see Fig. 1). Technically, the cutoff of the transverse momenta in these matrix elements is done by adding counterterms with normalization point μ^2.
- Find the evolution equations of light-ray operators with respect to μ^2.
- Solve of the corresponding evolution equation(s).
- Assemble the result for structure functions: take some initial conditions at low normalization point (usually around μ^2=1GeV^2), evolve parton densities to high Q^2 and multiply the result by the coefficient function.

Let me explain these steps at the NLO level in detail.

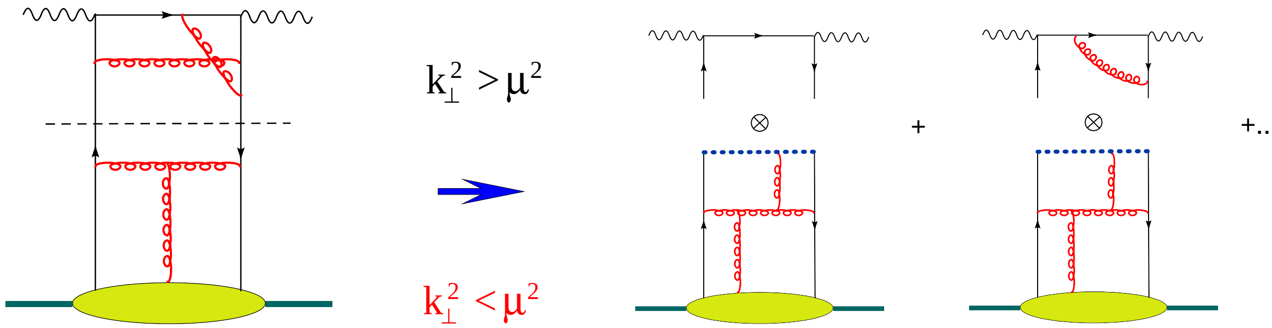

FIG. 1: Operator product expansion near the light cone. Gauge link is denoted by a dotted line.

One can calculate the coefficient functions by direct computation of Feynman diagrams with quark and gluon tails or by using the Feynman diagrams in external quark and gluon fields (see e.g. [20, 21]). A typical NLO contribution coming from the upper part of last diagram in Fig. 1 has the form

$$T\{j_\mu(x)j_\mu(0)\} \;=\; \frac{-i}{\pi^2x^4}\int_0^1 du\,\left[\frac{1}{u}\right]_+[\psi(x)[x,ux]\not{x}\psi(ux)]^{\rm l.t.}\Big(1+\frac{\alpha_s}{4\pi}[\ln x^2\mu^2+\ln u]\Big)+... \tag{13}$$

where $\left[\frac{1}{u}\right]_+$ is a standard "plus" prescription

$$\int_0^1 du\,\left[\frac{1}{u}\right]_+ f(u) \;\equiv\; \int_0^1 du\,\frac{f(u)-f(0)}{u} \tag{14}$$

and the leading-twist light-ray operator $[\psi(x)[x,ux]\not{x}\psi(ux)]^{\rm l.t.}$ is taken at $x^2=0$. Formally, one can consider the operator at $\tilde{x}$ where $\tilde{x}$ is close to x and light-like. Alternatively, one can define a "leading twist" prescription by subtraction of all higher twists in the non-local form, see [22]. In any case, the light-ray operator $[\psi(x)[x,ux]\not{x}\psi(ux)]^{\rm l.t.}$ has specific light-cone UV divergencies (in addition to usual UV contributions assembled to the running coupling constant) which are regularized by adding light-ray counterterms. The resulting composite operator (original operator minus counterterms) depends on the renormalization point μ and the renorm-group equation for these operators leads to the DGLAP evolution equation for parton densities.

A typical contribution to the NLO evolution equation of the quark light-ray operator coming from the bottom part of diagram in Fig. 1 has the form

$$\mu\frac{d}{d\mu}[\psi(x)[x,0]\not{x}\psi(0)]^\mu_{\rm l.t.} \;=\; \frac{\alpha_s(\mu)}{2\pi}c_F\int_0^1 du\,\left[\frac{1}{u}\right]_+[\psi(x)[x,ux]\not{x}\psi(ux)]^\mu_{\rm l.t.}\Big(1+\frac{\alpha_s}{4\pi}[\ln x^2\mu^2+\ln u]\Big)+... \tag{15}$$

($c_F=(N_c^2-1)/2N_c$). This completes the second step of the above four-step program.

The third step is the solution of the evolution equation of (15) type. I will present this solution in a simple case of forward matrix elements of quark operators for a non-singlet case determined by quark parton densities. For example, in the case of unpolarized proton we get

$$\langle p|[\bar{q}(x)[x,0]\not{x}q(0)-\bar{q}\,\not{x}[0,x]q(x)]^\mu_{\rm l.t.}|p\rangle \;=\; 2(px)\int_0^1 d\omega\;\mathcal{D}_q(\omega)\big[e^{ip\cdot x\omega}-e^{-ip\cdot x\omega}\big] \tag{16}$$

where p is the proton momentum and $D_q(\omega)$ is a parton density of quark q (u, d, or s). The solution of the evolution equation for parton densities is given by the Mellin integral. In terms of light-ray operators it has the form

$$\langle\psi(x)[x,0]\not{x}\lambda^a\psi(0)]^\mu_{\rm l.t.}\rangle \;=\; \int_{-\frac12-i\infty}^{-\frac12+i\infty}\frac{d\nu}{2\pi i}\Big(\frac{\alpha_s(\mu)}{\alpha_s(\mu_0)}\Big)^{\frac{-\gamma_j^{(1)}}{b}}e^{-\frac{\alpha_s(\mu)-\alpha_s(\mu_0)}{4\pi b}[\gamma_j^{(2)}+\gamma_j^{(1)}b_1]}\int_0^\infty du\;u^j\langle\psi(ux)[ux,0]\not{x}\lambda^a\psi(0)]^{\mu_0}_{\rm l.t.}\rangle \tag{17}$$

where λ^a is a flavor Gell-Mann matrix and $\langle\mathcal{O}\rangle$ means any forward matrix element of the operator $\mathcal{O}$. Also, $\gamma_j(\alpha_s)=\gamma_j^{(1)}\frac{\alpha_s}{4\pi}+\gamma_j^{(2)}\frac{\alpha_s^2}{16\pi^2}+...$ is the anomalous dimension of the light-ray operator $\int_0^\infty du\;u^j\psi(ux)[ux,0]\not{x}\lambda^a\psi(0)$ and b_1 is the second coefficient of Gell-Mann-Low function.

Now, to perform step four and get a structure function ($-3F_1 + \frac{1}{2}F_2$ in our case) one can take parton densities at low $\mu_0^2 \sim 1\mathrm{Gev}^2$, put it into Eq. (17), take $\mu^2 = Q^2$ and multiply the result by the coefficient function (13) taken at $\mu^2 = Q^2$. In future, one should get the parton densities at low μ^2 from non-perturbative (lattice) QCD but at present people use well established models. The evolution of parton densities in QCD is calculated up to the third order in α_s [5] and the results agree with experiment in a broad range of parameters Q^2 and x_B.

III. HIGH-ENERGY OPE IN WILSON LINES

Now we want to extend the four-step program from the previous section to describe the high-energy amplitudes. A typical process is deep inelastic scattering at small values of Bjorken x. Since we are interested now in x_B evolution rather than Q^2 evolution, as step one we factorize in rapidity instead of transverse momenta. As a preliminary step we identify the relevant operators. The virtual photon splits into quark-antiquark pair, and if we set formally the energy of incoming photon to infinity we see that these quark and antiquark travel along the light-like classical trajectories. This is the well-known general result from quantum mechanics - the fast particle moves along its straight-line classical trajectory and the only quantum effect is the eikonal phase factor acquired along this propagation path. In QCD, for fast quark or gluon scattering off some target, this eikonal phase factor is a Wilson line (5) - an infinite gauge link ordered along the straight line collinear to particle's velocity n^μ:

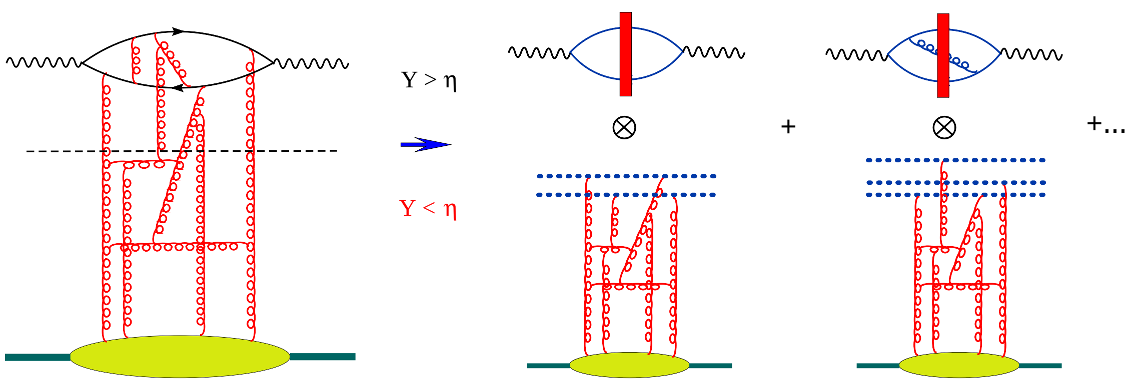

FIG. 2: High-energy operator expansion in Wilson lines

Having identified the operators, we can repeat the 4 steps which give us the high-energy (small-x for DIS) evolution of the amplitude.

- Separate the relevant Feynman loop integrals over the longitudinal momentum α in two parts - the coefficient functions ("impact factors") with α greater than the rapidity factorization scale $\sigma = e^\eta$ and matrix elements of Wilson-line operators with $\alpha < \sigma$ (see Fig. 2). We were not able to find the analog of dimensional regularization for longitudinal divergence so we cut the integration over $\alpha < \sigma$ " by hand".

- Find the evolution equations of color dipoles with respect to the cutoff in rapidity Y.

- Solve of the corresponding evolution equation(s).

- Assemble the result for structure functions: take the initial conditions at low energy, evolve color dipoles to high rapidity $Y \sim Y_A$ and multiply the result by the corresponding impact factor.

Unlike the DGLAP evolution discussed above, the BK evolution equation for color dipoles with respect to energy is non-linear which makes it considerably more difficult to solve. At present, for the experimentally interesting case of DIS from proton or nucleus we have no analytical solution so one has to rely upon the approximate solutions and numerical simulations. One can linearize the BK equation and get the usual linear BFKL evolution but the validity of this linearization in the saturation region of small x is questionable. Still, there are purely perturbative processes where the BFKL equation gives the correct (pre-asymptotic) behavior at high energies: for example the scattering of virtual photons with equal (and high) virtualities, or observation of two Mueller-Navelet jets [23] in hadron-hadron scattering. In this case, the leading-order analysis has been performed, but the generalizations of the LO results to the next-to-leading order has not been obtained since it is difficult to take into account the running-coupling effects in the BFKL equation.

By the same token, since in $\mathcal{N}=4$ SYM the coupling does not run, the NLO BFKL program can be performed to the very end. I will present the NLO analysis of high-energy "scattering of two scalar currents" and get the NLO result for this correlation function in an explicit form. In subsequent two chapters we will carry out steps (1-4) of our program for $\mathcal{N}=4$ SYM and then for QCD (where we'll discuss only steps 1 and 2).

IV. HIGH-ENERGY AMPLITUDES IN $\mathcal{N}=4$ SYM IN THE NEXT-TO-LEADING ORDER

A. Regge limit and Pomeron in $\mathcal{N}=4$ SYM

As we mentioned above, at first we will find the NLO amplitudes at high energies for $\mathcal{N}=4$ SYM and turn to QCD later. We use the $\mathcal{N}=4$ Lagrangian in the form (see e.g. Ref. [24]):

$$\begin{aligned}\mathcal{L} \;=\;& -\frac{1}{4}F^{\mu\nu}F_{\mu\nu}+\frac{1}{2}\big(D^\mu\Phi^a_I\big)\big(D_\mu\Phi^a_I\big)-\frac{1}{4}g^2f^{abc}f^{lmc}\Phi^a_I\Phi^b_J\Phi^l_I\Phi^m_J\\ &+\bar\lambda^a_{\dot\alpha A}\sigma^{\dot\alpha\beta}_\mu\mathcal{D}^\mu\lambda^{aA}_\beta-i\lambda^{\alpha A}_a\bar\Sigma^s_{AB}\Phi^s_b\lambda^B_{\alpha k}f^{abc}+i\bar\lambda^a_{\dot\alpha A}\Sigma^{sAB}\Phi^s_b\bar\lambda^{\dot\alpha}_{Bc}f^{abc}\end{aligned}\tag{18}$$

Here Φ^a_I are scalars, $\lambda^{\alpha A}_a$ gluinos and $\Sigma^a_{IJ}=(Y^i_{AB},i\bar Y^i_{AB})$, $\bar\Sigma^a_{IJ}=(Y^i_{AB},-i\bar Y^i_{AB})$ where Y^i_{AB} are standard 't Hooft symbols. The bare propagators are

$$\langle\Phi^a_I(x)\Phi^b_J(y)\rangle \;=\; i\delta^{ab}\delta_{IJ}\int d\!\!{}^-{}^4p\frac{e^{-ip\cdot(x-y)}}{-p^2+i\epsilon},\qquad \langle\lambda^{aI}_\beta(x)\,\bar\lambda^{bJ}_{\dot\alpha}(y)\rangle=\int d\!\!{}^-{}^4p\,e^{ip\cdot(x-y)}\frac{ip_\mu\,\bar\sigma^\mu_{\beta\dot\alpha}}{-p^2+i\epsilon},\tag{19}$$

and the vertex of gluon emission in the momentum space is proportional to $(k_1-k_2)^\mu T^a\delta_{IJ}$ for the scalars and $\sigma^\mu T^a$ for gluinos. Here $\sigma^\mu=(1,\vec\sigma)$, $\bar\sigma^\mu=(-1,\vec\sigma)$ where $\vec\sigma$ are usual Pauli matrices and our metric is $g^{\mu\nu}=(-1,1,1,1)$.

For simplicity, let us consider correlation function of four scalar currents

$$A(x,y,x',y') \;=\; (x-y)^4(x'-y')^4\langle\mathcal{O}(x)\mathcal{O}^\dagger(y)\mathcal{O}(x')\mathcal{O}^\dagger(y')\rangle\tag{20}$$

where $\mathcal{O}\equiv\frac{4\pi^2\sqrt2}{\sqrt{N_c^2-1}}\mathrm{Tr}\{\mathrm{Z}^2\}$ $(Z=\frac{1}{\sqrt2}(\Phi_1+i\Phi_2))$ is a renorm-invariant chiral primary operator.

In a conformal theory this four-point amplitude $A(x,y;x',y')$ depends on two conformal ratios which can be chosen as

$$R \;=\; \frac{(x-x')^2(y-y')^2}{(x-y)^2(x'-y')^2},\qquad\qquad r \;=\; R\Big[1-\frac{(x-y')^2(y-x')^2}{(x-x')^2(y-y')^2}+\frac{1}{R}\Big]^2\tag{21}$$

We are interested in the behavior of the correlator (20) in the high-energy (Regge) limit. In the coordinate space it can be achieved as follows:

$$x=\rho x_*\frac{2}{s}p_1+x_\perp,\quad y=\rho y_*\frac{2}{s}p_1+y_\perp,\qquad\qquad x'=\rho' x'_\bullet\frac{2}{s}p_2+x'_\perp,\quad y'=\rho' y'_\bullet\frac{2}{s}p_2+y'_\perp\tag{22}$$

with $\rho,\rho'\to\infty$ and $x_*>0>y_*$, $x'_\bullet>0>y'_\bullet$. (Strictly speaking, $\rho\to\infty$ or $\rho'\to\infty$ would be sufficient to reach the Regge limit). Hereafter I use the notations $x_\bullet=-p_1^\mu x_\mu$, $x_*=-p_2^\mu x_\mu$ where p_1 and p_2 are light-like vectors normalized by $-2(p_1,p_2)=s$. These "Sudakov variables" are related to the usual light-cone coordinates $x^\pm=\frac{1}{\sqrt2}(x^0\pm x^3)$ by $x_*=x^+\sqrt{s/2}$, $x_\bullet=x^-\sqrt{s/2}$ so $x=\frac{2}{s}x_*p_1+\frac{2}{s}x_\bullet p_2+x_\perp$. The metric is $g^{\mu\nu}$=(-1,1,1,1) so $x^2=-\frac{4}{s}x_\bullet x_*+\vec x_\perp^2$. In the Regge limit (22) the full conformal group reduces to Möbius subgroup SL(2,C) leaving the transverse plane $(0,0,z_\perp)$ invariant.

As demonstrated in Ref. [25], the pomeron contribution in a conformal theory can be represented as an integral over one real variable ν

$$(x-y)^4(x'-y')^4\langle\mathcal{O}(x)\mathcal{O}^\dagger(y)\mathcal{O}(x')\mathcal{O}^\dagger(y')\rangle \;=\; \frac{i}{2}\int d\nu\;\tilde f_+(\nu)\frac{\tanh\pi\nu}{\nu}F(\nu)\Omega(r,\nu)R^{\frac12\omega(\nu)}\tag{23}$$

Here $\omega(\nu)\equiv\omega(0,\nu)$ is the pomeron intercept, $\tilde f_+(\nu)\equiv\tilde f_+(\omega(\nu))$ where $\tilde f_+(\omega)=(e^{i\pi\omega}-1)/\sin\pi\omega$ is the signature factor in the coordinate space, and $F(\nu)$ is the "pomeron residue" (strictly speaking, the product of two pomeron residues). The conformal function $\Omega(r,\nu)$ is given by a hypergeometric function (see Ref. [26]) but for our purposes it is convenient to use the representation in terms of the two-dimensional integral

$$\Omega(r,\nu) \;=\; \frac{\nu^2}{\pi^3}\int d^2z\Big[\frac{-\kappa^2}{(-2\kappa\cdot\zeta)^2}\Big]^{\frac12+i\nu}\Big[\frac{-\kappa'^2}{(-2\kappa'\cdot\zeta)^2}\Big]^{\frac12-i\nu}\tag{24}$$

where $\zeta \equiv \frac{p_1}{s} + z_\perp^2 p_2 + z_\perp$ and

$$\kappa = \frac{\sqrt{s}}{2x_*}(\frac{p_1}{s} + x^2 p_2 + x_\perp) - \frac{\sqrt{s}}{2y_*}(\frac{p_1}{s} + y^2 p_2 + y_\perp) \tag{25}$$
$$\kappa' = \frac{\sqrt{s}}{2x'_\bullet}(\frac{p_1}{s} + {x'}^2 p_2 + x'_\perp) - \frac{\sqrt{s}}{2y'_\bullet}(\frac{p_1}{s} + {y'}^2 p_2 + y'_\perp)$$

are two SL(2,C)-invariant vectors [26] (see also [27]) such that $\kappa^2 = \frac{s(x-y)^2}{4x_* y_*}$, ${\kappa'}^2 = \frac{s(x'-y')^2}{4x'_\bullet y'_\bullet}$ and therefore

$$\kappa^2 {\kappa'}^2 = \frac{1}{R}, \qquad 4(\kappa\cdot\kappa')^2 = \frac{r}{R} \tag{26}$$

In our limit (22) $x^2 = x_\perp^2$, ${x'}^2 = {x'}_\perp^2$ and similarly for y. Note that all the dependence on large energy ($\equiv$ large ρ, ρ') is contained in $R^{\frac{1}{2}\omega(\nu)}$.

The dynamical information about the conformal theory is encoded in two functions: pomeron intercept and pomeron residue. The pomeron intercept is known both in the small and large α_s limit. The NLO intercept at small α_s was calculated in $\mathcal{N}=4$ SYM by Lipatov and Kotikov [28]

$$\omega(\nu) = \frac{\alpha_s}{\pi} N_c\Big(\chi(\nu) + \frac{\alpha_s N_c}{4\pi}\Big[6\zeta(3) - \frac{\pi^2}{3}\chi(\nu) + \chi''(\nu) - 2\Phi(\nu) - 2\Phi(-\nu)\Big]\Big) \tag{27}$$

Our main goal is the description of the amplitude in the next-to-leading order in perturbation theory, but it is worth noting that the pomeron intercept is known also in the limit of large 't Hooft coupling $\lambda = 4\pi\alpha_s N_c$

$$\omega(\nu) + 1 = j(\nu) = 2 - 2\frac{\nu^2+1}{\sqrt{\lambda}} \tag{28}$$

where 2 is the graviton spin and the first correction was calculated in Ref. [29, 30].

The pomeron residue $F(\nu)$ is known in the leading order both at small [26, 31, 32] and large [25] 't Hooft coupling

$$F(\nu) \overset{\lambda\to 0}{\to} \lambda^2 \frac{\pi\sin\pi\nu}{4\nu\cos^3\pi\nu}, \qquad F(\nu) \overset{\lambda\to\infty}{\to} \frac{\pi^3\nu^2(1+\nu)^2}{\sinh^2\pi\nu} \tag{29}$$

To find the NLO amplitude, we must also calculate the "pomeron residue" $F(\nu)$ in the next-to-leading order. In the rest of this section we will do this using the four steps of the high-energy operator product expansion in Wilson lines.

B. High-energy OPE in the leading order

1. Leading order: impact factor

As I discussed above, the main idea behind the high-energy operator expansion is the rapidity factorization. At the first step, we integrate over gluons with rapidities $Y > \eta$ and leave the integration over $Y < \eta$ for later time, see Fig. 2. It is convenient to use the background field formalism: we integrate over gluons with $\alpha > \sigma$ and leave gluons with $\alpha < \sigma$ as a background field, to be integrated over later. The result of the integration is the coefficient function ("impact factor") in front of the Wilson-line operators with rapidities up to $\eta = \ln\sigma$:

$$U^\sigma_x = \mathrm{Pexp}\Big[-ig\int_{-\infty}^{\infty} du\; p_1^\mu A^\sigma_\mu(up_1 + x_\perp)\Big], \qquad A^\sigma_\mu(x) = \int d^4k\;\theta(\sigma - |\alpha_k|)e^{ik\cdot x}A_\mu(k) \tag{30}$$

where the Sudakov variable α_k is defined as usual, $k = \alpha_k p_1 + \beta_k p_2 + k_\perp$. The impact factor is given then by a set of Feynman diagrams in the external field of gluons with $\alpha < \sigma$. Since the rapidities of the background gluons are very different from the rapidities of gluons in our Feynman diagrams, the background field can be taken in a form of the shock wave due to the Lorentz contraction. It is very easy to derive the expression of a quark (or gluon) propagator in this shock-wave background. We represent the propagator as a path integral over various trajectories, each of them weighed with the gauge factor $\mathrm{Pexp}(ig\int dx_\mu A^\mu)$ ordered along the propagation path. Now, since the shock wave is very thin, quarks (or gluons) do not have time to deviate in transverse direction so their trajectory inside the shock wave can be approximated by a segment of the straight line. Morover, since there is no external field outside the

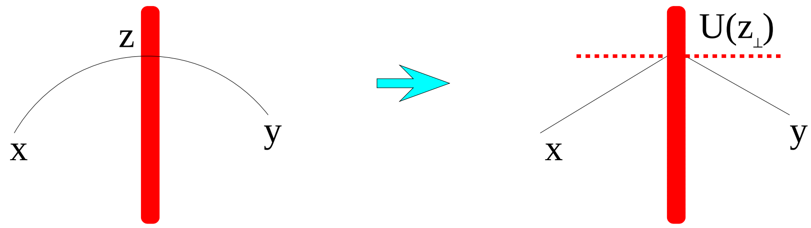

FIG. 3: Propagator in a shock-wave background

shock wave [43] the integral over the segment of straight line can be formally extended to $\pm\infty$ limits yielding the Wilson-line operator.

Thus, the structure of the propagator in a shock-wave background is as follows:
$\big[$Free propagation from initial point x to the point of intersection with the shock wave $z\big]$
$\times$ $\big[$Interaction with the shock wave described by the Wilson-line operator $U_z\big]$
$\times$ $\big[$Free propagation from point of interaction z to the final point $y\big]$.

The explicit form can be taken from Ref. [14]

$$\begin{aligned}\langle\hat{\Phi}_I(x)\hat{\Phi}_J(y)\rangle_{\rm shockwave} &\stackrel{x_*>0>y_*}{=} 2i\delta^{IJ}\int d^4z\,\delta(z_*)\frac{1}{4\pi^2[(x-z)^2+i\epsilon]}\,U^{ab}_{z_\perp}\,\partial_*^{(z)}\frac{1}{4\pi^2[(z-y)^2+i\epsilon]}\\ &= \frac{s^2\delta^{IJ}}{64\pi^3x_*y_*}\int_0^\infty d\alpha\;\alpha e^{i\alpha\frac{s}{4}\mathcal{Z}} \;=\; -\frac{\delta^{IJ}}{4\pi^3x_*y_*\mathcal{Z}^2}\end{aligned}\tag{31}$$

where $\mathcal{Z}\equiv-\frac{4}{\sqrt{s}}(\kappa\cdot\zeta)=-\frac{4}{s}(x-y)_\bullet+\frac{(x-z)^2_\perp}{x_*}-\frac{(y-z)^2_\perp}{y_*}$. Note that the interaction with the shock wave does not change the α-component of the scalar particle's momentum.

Let us calculate the impact factor taking $x_\bullet=y_\bullet=0$ for simplicity. The leading-order impact factor is proportional to the product of two propagators (31), see Fig. 4:

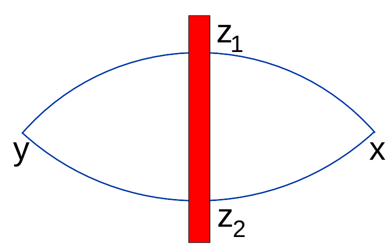

FIG. 4: Impact factor in the leading order.

$$\langle T\{\hat{\mathcal{O}}(x)\hat{\mathcal{O}}(y)\}\rangle^{\rm LO}_{\rm shockwave} \;=\; \frac{(x-y)^{-4}}{\pi^2(N_c^2-1)}\int\frac{d^2z_{1\perp}d^2z_{2\perp}}{z_{12}^4}\;\mathcal{R}^2\;{\rm Tr}\{U_{z_1}U^\dagger_{z_2}\}\tag{32}$$

where

$$\mathcal{R} \;=\; -\frac{(x-y)^2z_{12}^2}{x_*y_*\mathcal{Z}_1\mathcal{Z}_2} \;=\; \frac{\kappa^2(\zeta_1\cdot\zeta_2)}{2(\kappa\cdot\zeta_1)(\kappa\cdot\zeta_2)}\tag{33}$$

and $\zeta_i\equiv\frac{p_1}{s}+z_i^2p_2+z_i^\perp$, $\mathcal{Z}_i\equiv-\frac{4}{\sqrt{s}}(\kappa\cdot\zeta_i)=\frac{(x-z_i)^2}{x_*}-\frac{(y-z_i)^2}{y_*}$. Note that the leading-order impact factor is conformally (Möbius) invariant - it goes into itself under the inversion (10).

This formula can be promoted to the operator equation as follows

$$(x-y)^4T\{\hat{\mathcal{O}}(x)\hat{\mathcal{O}}(y)\}^{\rm LO} \;=\; \frac{1}{\pi^2(N_c^2-1)}\int\frac{d^2z_1d^2z_2}{z_{12}^4}\;\mathcal{R}^2\;{\rm Tr}\{\hat{U}^{\sigma_A}_{z_1}\hat{U}^{\dagger\sigma_A}_{z_2}\}\tag{34}$$

where $\sigma_A\sim\frac{\sqrt{x_*|y_*|}}{s(x-y)^2}$ is the characteristic $\alpha's$ in the scalar loop which serve as an upper bound for rapidity of Wilson-line gluons. (Recall that $|y_*|$ and x_* are of the same order of magnitude as seen from Eq. (22)).

We'll need later the projection of the T-product in the l.h.s. of this equation onto the conformal eigenfunctions of the BFKL equation [15]

$$E_{\nu,n}(z_{10},z_{20}) \;=\; \Big[\frac{\tilde z_{12}}{\tilde z_{10}\tilde z_{20}}\Big]^{\frac12+i\nu+\frac{n}{2}}\Big[\frac{\bar z_{12}}{\bar z_{10}\bar z_{20}}\Big]^{\frac12+i\nu-\frac{n}{2}} \tag{35}$$

(here $\tilde z = z_x + iz_y, \bar z = z_x - iz_y$, $z_{10}\equiv z_1 - z_0$ etc.). Since $\hat{\mathcal{O}}$'s are scalar operators, the only non-vanishing contribution comes from projection on the eigenfunctions with spin 0:

$$\frac{1}{\pi^2}\int\frac{dz_1dz_2}{z_{12}^4}\,\mathcal{R}^2\Big[\frac{z_{12}^2}{z_{10}^2z_{20}^2}\Big]^{\frac12+i\nu} \;=\; \Big[\frac{-\kappa^2}{(-2\kappa\cdot\zeta_0)^2}\Big]^{\frac12+i\nu}\frac{\Gamma^2\big(\frac12-i\nu\big)}{\Gamma(1-2i\nu)}\frac{\big(\frac14+\nu^2\big)\pi}{\cosh\pi\nu} \tag{36}$$

where $\zeta_0\equiv\frac{p_1}{s}+z_{0\perp}^2p_2+z_{0\perp}$.

Now, using the decomposition of the product of the transverse δ-functions in conformal 3-point functions $E_{\nu,n}(z_{10},z_{20})$ [15]

$$\delta^{(2)}(z_1-w_1)\delta^{(2)}(z_2-w_2) \;=\; \sum_{n=-\infty}^{\infty}\int\frac{d\nu}{\pi^4}\,\frac{\nu^2+\frac{n^2}{4}}{z_{12}^2w_{12}^2}\int d^2\rho\;E^*_{\nu,n}(w_1-\rho,w_2-\rho)E_{\nu,n}(z_1-\rho,z_2-\rho) \tag{37}$$

we obtain (dots stand for contributions of higher spins n which we do not need for our correlator (20))

$$(x-y)^4T\{\hat{\mathcal{O}}(x)\hat{\mathcal{O}}^\dagger(y)\} \;=\; -\int d\nu\int d^2z_0\;\frac{\nu^2(1+4\nu^2)}{4\pi\cosh\pi\nu}\frac{\Gamma^2\big(\frac12-i\nu\big)}{\Gamma(1-2i\nu)}\;\Big(\frac{-\kappa^2}{(-2\kappa\cdot\zeta_0)^2}\Big)^{\frac12+i\nu}\hat{\mathcal{U}}^{\sigma_A}(\nu,z_0)\;+\;... \tag{38}$$

where

$$\hat{\mathcal{U}}^\sigma(\nu,z_0)\;\equiv\;\frac{1}{\pi^2}\int\frac{d^2z_1d^2z_2}{z_{12}^4}\;\Big(\frac{z_{12}^2}{z_{10}^2z_{20}^2}\Big)^{\frac12-i\nu}\;\hat{\mathcal{U}}^\sigma(z_1,z_2) \tag{39}$$

and $\hat{\mathcal{U}}^\sigma(z_1,z_2)$ is a "color dipole in the adjoint representation"

$$\hat{\mathcal{U}}^\sigma(z_1,z_2)\;=\;1-\frac{1}{N_c^2-1}\mathrm{Tr}\{\hat U^\sigma_{z_1}\hat U^{\dagger\sigma}_{z_2}\} \tag{40}$$

2. Leading order: BK equation

Next step is to obtain the evolution equation for color dipoles in the leading order in α_s. For the light-cone dipoles, the contribution of scalar operators to Maldacena-Wilson line [16] vanishes so one has the usual Wilson line constructed from gauge fields and therefore the LLA evolution equation for color dipoles in the $\mathcal{N}=4$ SYM has the same form as in QCD.

To find the evolution of the color dipole (6) with respect to rapidity of the Wilson lines in the leading log approximation we consider the matrix element of the color dipole between (arbitrary) target states and integrate over the gluons with rapidities $Y_1 > Y > Y_2 = Y_1 - \Delta Y$ leaving the gluons with $Y < Y_2$ as a background field (to be integrated over later). In the frame of gluons with $Y \sim Y_1$ the fields with $Y < Y_2$ shrink to a pancake and we obtain the four diagrams shown in Fig. 5. Technically, to find the kernel in the leading-ordrer approximation we write down the general form of the operator equation for the evolution of the color dipole

$$\frac{d}{dY}\mathrm{Tr}\{\hat U^Y_{z_1}\hat U^{\dagger Y}_{z_2}\} = K_{\mathrm{LO}}\mathrm{Tr}\{\hat U^Y_{z_1}\hat U^{\dagger Y}_{z_2}\}+... \tag{41}$$

(where dots stand for the higher orders of the expansion) and calculate the l.h.s. of Eq. (41) in the shock-wave background

$$\frac{d}{dY}\langle\mathrm{Tr}\{\hat U^Y_{z_1}\hat U^{\dagger Y}_{z_2}\}\rangle_{\mathrm{shockwave}} = \langle K_{\mathrm{LO}}\mathrm{Tr}\{\hat U^Y_{z_1}\hat U^{\dagger Y}_{z_2}\}\rangle_{\mathrm{shockwave}} \tag{42}$$

In what follows we replace $\langle...\rangle_{\mathrm{shockwave}}$ by $\langle...\rangle$ for brevity.

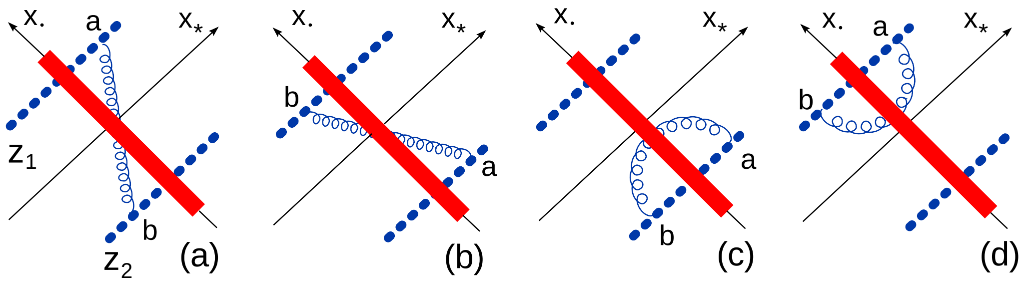

FIG. 5: Leading-order diagrams for the small-x evolution of color dipole. Gauge links are denoted by dotted lines.

With future NLO computation in view, we will perform the leading-order calculation in the lightcone gauge $p_2^\mu A_\mu = 0$. The gluon propagator in a shock-wave external field has the form[17, 33]

$$\langle \hat{A}^a_\mu(x)\hat{A}^b_\nu(y)\rangle \stackrel{x_*>0>y_*}{=} -\frac{i}{2}\int d^4z\ \delta(z_*)\ \frac{x_* g^\perp_{\mu\xi} - p_{2\mu}(x-z)^\perp_\xi}{\pi^2[(x-z)^2+i\epsilon]^2}\ U^{ab}_{z_\perp}\frac{1}{\partial^{(z)}_*}\ \frac{y_*\delta^{\perp\xi}_\nu - p_{2\nu}(y-z)^\xi_\perp}{\pi^2[(z-y)^2+i\epsilon]^2} \tag{43}$$

where $\frac{1}{\partial_*}$ can be either $\frac{1}{\partial_*+i\epsilon}$ or $\frac{1}{\partial_*-i\epsilon}$ which leads to the same result. (This is obvious for the leading order and correct in NLO after subtraction of the leading-order contribution, see Eq. (67) below).

We obtain

$$g^2\int_0^\infty du\int_{-\infty}^0 dv\ \langle \hat{A}^{a,Y_1}_\bullet(up_1+x_\perp)\hat{A}^{b,Y_1}_\bullet(vp_1+y_\perp)\rangle_{\rm Fig.5a} = -4\alpha_s\int_0^{e^{Y_1}}\frac{d\alpha}{\alpha}(x_\perp|\frac{p_i}{p^2_\perp-i\epsilon}U^{ab}\frac{p_i}{p^2_\perp-i\epsilon}|y_\perp) \tag{44}$$

Hereafter we use Schwinger's notations $(x_\perp|F(p_\perp)|y_\perp) \equiv \int \not{d}p\ e^{i(p,x-y)_\perp}F(p_\perp)$ (the scalar product of the four-dimensional vectors in our notations is $x\cdot y = -\frac{2}{s}(x_*y_\bullet + x_*y_\bullet) + (x,y)_\perp$). Note that the interaction with the shock wave does not change the α-component of the gluon momentum, same as for the scalar propagator (31)

Formally, the integral over α diverges at the lower limit, but since we integrate over the rapidities $Y > Y_2$ in the leading log approximation, we get ($\Delta Y \equiv Y_1 - Y_2$)

$$g^2\int_0^\infty du\int_{-\infty}^0 dv\ \langle \hat{A}^{a,Y_1}_\bullet(up_1+x_\perp)\hat{A}^{b,Y_1}_\bullet(vp_1+y_\perp)\rangle_{\rm Fig.5a} = -4\alpha_s\Delta Y(x_\perp|\frac{p_i}{p^2_\perp}U^{ab}\frac{p_i}{p^2_\perp}|y_\perp) \tag{45}$$

and therefore

$$\langle \hat{U}^Y_{z_1}\otimes\hat{U}^{\dagger Y}_{z_2}\rangle^{Y_1}_{\rm Fig.5a} = -\frac{\alpha_s}{\pi^2}\Delta Y\ (T^aU_{z_1}\otimes T^bU^\dagger_{z_2})\int d^2z_3\frac{(z_{13},z_{23})}{z^2_{13}z^2_{23}}U^{ab}_{z_3} \tag{46}$$

(hereafter $T^a_{mn}\equiv -if^{amn}$). The contribution of the diagram in Fig. 5b is obtained from Eq. (46) by the replacement $T^aU_{z_1}\otimes T^bU^\dagger_{z_2}\to U_{z_1}T^b\otimes U^\dagger_{z_2}T^a$, $z_2\leftrightarrow z_1$ and the two remaining diagrams are obtained from Eq. 45 by taking $z_2 = z_1$ (Fig. 5c) and $z_1 = z_2$ (Fig. 5d). Finally, one has

$$\langle {\rm Tr}\{\hat{U}^{Y_1}_{z_1}\hat{U}^{\dagger Y_1}_{z_2}\}\rangle_{\rm Fig.5} = \frac{\alpha_s\Delta Y}{\pi^2}\int d^2z_3\frac{z^2_{12}}{z^2_{13}z^2_{23}}[{\rm Tr}\{T^aU_{z_1}U^\dagger_{z_3}T^aU_{z_3}U^\dagger_{z_2}\} - \frac{1}{N_c}{\rm Tr}\{U_{z_1}U^\dagger_{z_2}\}] \tag{47}$$

There are also contributions coming from diagrams similar to Fig. 5 but without the gluon-shockwave intersection. These diagrams are proportional to the original dipole ${\rm Tr}\{U_{z_1}U^\dagger_{z_2}\}$ and therefore the corresponding term can be derived from the contribution of Fig. 5 graphs using the requirement that the r.h.s. of the evolution equation should vanish in the absence of the shock wave (when $U\equiv 1$). It is easy to see that this requirement leads to

$$\langle {\rm Tr}\{\hat{U}^{Y_1}_{z_1}\hat{U}^{\dagger Y_1}_{z_2}\}\rangle = \frac{\alpha_s\Delta Y}{\pi^2}\int d^2z_3\frac{z^2_{12}}{z^2_{13}z^2_{23}}[{\rm Tr}\{T^aU_{z_1}U^\dagger_{z_3}T^aU_{z_3}U^\dagger_{z_2}\} - N_c{\rm Tr}\{U_{z_1}U^\dagger_{z_2}\}]$$

which gives the BK equation for the evolution of the color dipole in the adjoint representation:.

$$\frac{d}{dY}{\rm Tr}\{\hat{U}^Y_{z_1}\hat{U}^{\dagger Y}_{z_2}\} = \frac{\alpha_s}{\pi^2}\int d^2z_3\frac{z^2_{12}}{z^2_{13}z^2_{23}}[{\rm Tr}\{T^a\hat{U}^Y_{z_1}\hat{U}^{\dagger Y}_{z_3}T^a\hat{U}^Y_{z_1}\hat{U}^{\dagger Y}_{z_2}\} - N_c{\rm Tr}\{\hat{U}^Y_{z_1}\hat{U}^{\dagger Y}_{z_2}\}] \tag{48}$$

3. Leading order: BFKL evolution of color dipoles

Next step is the evolution of color dipole. To find the amplitude (20) in the leading order (and NLO as well) it is sufficient to take into account only the linear evolution of Wilson-line operators which corresponds to taking into account only two gluons in the t-channel. The non-linear effects in the evolution (and the production) of t-channel gluons enter the four-current amplitude (20) in the form of so-called "pomeron loops" which start from the NNLO BFKL order. With this two-gluon accuracy

$$\frac{1}{N_c}\mathrm{Tr}\{T^n\hat{U}^\sigma_{z_1}\hat{U}^{\dagger\sigma}_{z_3}T^n\hat{U}^\sigma_{z_3}\hat{U}^{\dagger\sigma}_{z_2}\}-\mathrm{Tr}\{\hat{U}^\sigma_{z_1}\hat{U}^{\dagger\sigma}_{z_2}\} ~=~ -\frac{1}{2}(N_c^2-1)\big[\hat{\mathcal{U}}^\sigma(z_1,z_3)+\hat{\mathcal{U}}^\sigma(z_2,z_3)-\hat{\mathcal{U}}^\sigma(z_1,z_2)\big]$$

where $\hat{\mathcal{U}}^\sigma(z_1,z_2)$ is a color dipole in the adjoint representation, see Eq. (40). The BFKL equation for $\hat{\mathcal{U}}^\sigma(z_1,z_2)$ takes the form (recall that $\sigma=e^Y$)

$$\sigma\frac{d}{d\sigma}\hat{\mathcal{U}}^\sigma(z_1,z_2) ~=~ \int d^2z_3d^2z_4K_{\mathrm{LO}}(z_1,z_2;z_3,z_4)\,\hat{\mathcal{U}}^\sigma(z_3,z_4) \tag{49}$$

where

$$K_{\mathrm{LO}}(z_1,z_2;z_3,z_4) ~=~ \frac{\alpha_sN_c}{2\pi^2}\Big[\frac{z_{12}^2\delta^2(z_{13})}{z_{14}^2z_{24}^2}+\frac{z_{12}^2\delta^2(z_{24})}{z_{13}^2z_{23}^2}-~\delta^2(z_{13})\delta^2(z_{24})\int d^2z~\frac{z_{12}^2}{(z_1-z)^2(z_2-z)^2}\Big] \tag{50}$$

The solution of this equation is easily formulated in terms of $\hat{\mathcal{U}}^\sigma(\nu,z_0)$ - projection of color dipole on Lipatov's eigenfunctions (35):

$$\hat{\mathcal{U}}^\sigma(\nu,z_0) ~=~ (\sigma/\sigma_0)^{\omega(\nu)}\hat{\mathcal{U}}^{\sigma_0}(\nu,z_0) \tag{51}$$

4. LO: amplitude

The last step is a matrix element of the color dipole operator $\hat{\mathcal{U}}^{\sigma_0}(\nu,z_0)$ "between scalar states", i.e. the correlator of color dipole and "bottom pair" of scalar operators $\mathcal{O}(x')$ and $\mathcal{O}(y')$ in the leading order in perturbation theory. The easiest way to get this matrix element is to write down the high-energy OPE for the bottom pair of operators similar to Eq. (29)

$$(x'-y')^4T\{\hat{\mathcal{O}}(x')\hat{\mathcal{O}}^\dagger(y')\} ~=~ -\int d\nu'\int d^2z_0'~\frac{\nu'^2(1+4\nu'^2)}{4\pi\cosh\pi\nu'}\frac{\Gamma^2\big(\frac{1}{2}-i\nu'\big)}{\Gamma(1-2i\nu')}\Big(\frac{-\kappa'^2}{(-2\kappa'\cdot\zeta_0')^2}\Big)^{\frac{1}{2}+i\nu'}\hat{\mathcal{V}}^{\lambda_B}(\nu',z_0'). \tag{52}$$

Here $\zeta_0'\equiv p_1+\frac{z_0'^2}{s}p_2+z'_{0\perp}$, $b_0=\kappa'^{-2}+i\epsilon=\frac{4x'_\bullet y'_\bullet}{s(x'-y')^2}+i\epsilon$, and

$$\hat{\mathcal{V}}^\lambda(\nu',z_0') ~=~ \frac{1}{\pi^2}\int\frac{d^2z_1d^2z_2}{z_{12}^4}~\Big(\frac{z_{12}^2}{z_{10}^2z_{20}^2}\Big)^{\frac{1}{2}-i\nu'}~\hat{\mathcal{V}}^\lambda(z_1,z_2), \tag{53}$$

where the operator is made from the dipoles $\hat{\mathcal{V}}^\lambda(z_1',z_2') ~=~ 1-\frac{1}{N_c^2-1}\mathrm{Tr}\{\hat{V}^\lambda_{z_1'}\hat{V}^{\dagger\lambda}_{z_2'}\}$ (cf. Eq. (40)) ordered along the straight line $\parallel~p_2$ with the rapidity restriction

$$V^\lambda_x ~=~ \mathrm{Pexp}\Big[-ig\int_{-\infty}^{\infty}du~p_1^\mu A^\lambda_\mu(up_2+x_\perp)\Big],\qquad\qquad A^\lambda_\mu(x) ~=~ \int d^4k~\theta(\lambda-|\beta_k|)e^{ik\cdot x}A_\mu(k) \tag{54}$$

Similarly to the case of the upper impact factor discussed above, the cutoff λ for β integration in Eq. (54) should be chosen of order of characteristic β's in the lower impact factor so $\lambda_B\sim\frac{\sqrt{x'_\bullet|y'_\bullet|}}{s(x'-y')^2}$.

In the leading order in perturbation theory

$$\langle\mathcal{U}(z_1,z_2)\mathcal{V}(w_1,w_2)\rangle ~=~ -\frac{\alpha_s^2\pi^2N_c^2}{2(N_c^2-1)}\ln^2\frac{(z_1-w_1)^2(z_2-w_2)^2}{(z_1-w_2)^2(z_2-w_1)^2} \tag{55}$$

which will be true in the LLA as long as the α and β cutoffs do not allow large logarithms $\ln\frac{\alpha\beta s}{k_\perp^2}$ where $k_\perp^2$ is characteristic transverse momentum in gluon ladder describing the BFKL evolution. (This is similar to taking μ^2

around 1 GeV for the initial point of the DGLAP evolution so the logarithms $\ln\frac{\mu^2}{m_p^2}$ can be neglected). Thus, if we choose the final point of evolution (51) to be $\sigma_0 \sim \frac{k_\perp^2}{\lambda_B s} \sim (|x-y|_\perp|x'-y'|_\perp\lambda_B s)^{-1}$, the correlator of color dipoles $\langle\mathcal{U}^{\sigma_0}(z_1,z_2)\mathcal{V}^{\lambda_B}(w_1,w_2)\rangle$ will be given by Eq. (55) which translates to

$$\langle\hat{\mathcal{U}}^{\sigma_0}(\nu,z_0)\hat{\mathcal{V}}^{\lambda_B}(\nu',z_0')\rangle \;=\; -\frac{\alpha_s^2N_c^2}{N_c^2-1}\frac{16\pi^2}{\nu^2(1+4\nu^2)^2}\Big[\delta(z_0-z_0')\delta(\nu+\nu')+\frac{2^{1-4i\nu}\delta(\nu-\nu')}{\pi|z_0-z_0'|^{2-4i\nu}}\frac{\Gamma\big(\frac12+i\nu\big)\Gamma(1-i\nu)}{\Gamma(i\nu)\Gamma\big(\frac12-i\nu\big)}\Big] \tag{56}$$

where we used the following orthogonality condition for the eigenfunctions (35), see Ref. [15]:

$$\int\frac{d^2z_1d^2z_2}{z_{12}^4}\;E^*_{\nu',m}(z_1-z_0',z_2-z_0')E_{\nu,n}(z_1-z_0,z_2-z_0) \;=\; \frac{\pi^4}{2\big(\nu^2+\frac{n^2}{4}\big)}\Bigg[\delta(\nu-\nu')\delta_{m,n}\delta^{(2)}(z_0-z_0') \tag{57}$$
$$+\;\delta(\nu+\nu')\delta_{m,-n}(\tilde z_0-\tilde z_0')^{-1+n-2i\nu}(\bar z_0-\bar z_0')^{-1-n-2i\nu}\frac{2^{4i\nu+1}}{\pi}\Big(\frac{|n|}{2}+i\nu\Big)\frac{\Gamma\big(\frac{1+|n|}{2}-i\nu\big)\Gamma\big(\frac{|n|}{2}+i\nu\big)}{\Gamma\big(\frac{1+|n|}{2}+i\nu\big)\Gamma\big(\frac{|n|}{2}-i\nu\big)}\Bigg]$$

With our choice of σ_0 for the endpoint of the evolution of the color dipole (51) the correlator of two color dipoles $\hat{\mathcal{U}}^{\sigma_A}(\nu,z_0)$ and $\hat{\mathcal{V}}^{\lambda_B}(\nu',z_0')$ takes the form

$$\langle\hat{\mathcal{U}}^{\sigma_A}(\nu,z_0)\hat{\mathcal{V}}^{\lambda_B}(\nu',z_0')\rangle \tag{58}$$
$$=\;-\frac{\alpha_s^2N_c^2}{N_c^2-1}\frac{32\pi^2}{\nu^2(1+4\nu^2)^2}\Big(\frac{x_*y_*x_\bullet y_\bullet}{s(x-y)_\perp^2(x'-y')_\perp^2}\Big)^{\frac{\omega(\nu)}{2}}\Big[\delta(z_0-z_0')\delta(\nu+\nu')+\frac{2^{1-4i\nu}\delta(\nu-\nu')}{\pi|z_0-z_0'|^{2-4i\nu}}\frac{\Gamma\big(\frac12+i\nu\big)\Gamma(1-i\nu)}{\Gamma(i\nu)\Gamma\big(\frac12-i\nu\big)}\Big].$$

Combining now Eqs. (38), (52), and the above equation we see that the leading-order amplitude is given by Eq. (23) with $\omega_0(\nu)=\frac{\alpha_2N_c}{\pi}\chi(\nu)$ and

$$F_0(\nu) \;=\; \frac{N_c^2}{N_c^2-1}\frac{4\pi^4\alpha_s^2}{\cosh^2\pi\nu} \tag{59}$$

which agrees with the leading-order impact factor calculated in Refs. [26, 31]. Here we used the integral

$$\int\frac{d^2z_0'}{[(z_0-z_0')^2]^{1-2i\nu}}\Big[\frac{-\kappa'^2}{(-2\kappa'\cdot\zeta_0')^2}\Big]^{\frac12+i\nu} \;=\; \frac{\pi}{2i\nu}\Big[\frac{-\kappa'^2}{(-2\kappa'\cdot\zeta_0)^2}\Big]^{\frac12-i\nu} \tag{60}$$

C. NLO: Rapidity factorization

Now we repeat the same four steps of operator expansion at the NLO accuracy. A general form of the expansion of T-product of the currents $\mathcal{O}(x)$ and $\mathcal{O}(y)$ in color dipoles looks as follows:

$$T\{\hat{\mathcal{O}}(x)\hat{\mathcal{O}}(y)\} \;=\; \int d^2z_1d^2z_2\;I^{\rm LO}(z_1,z_2){\rm Tr}\{\hat U^Y_{z_1}\hat U^{\dagger Y}_{z_2}\}$$
$$+\int d^2z_1d^2z_2d^2z_3\;I^{\rm NLO}(z_1,z_2,z_3)[{\rm Tr}\{T^n\hat U^Y_{z_1}\hat U^{\dagger Y}_{z_3}T^n\hat U^Y_{z_3}\hat U^{\dagger Y}_{z_2}\}-N_c{\rm Tr}\{\hat U^Y_{z_1}\hat U^{\dagger Y}_{z_2}\}] \tag{61}$$

(structure of the NLO contribution is clear from the topology of diagrams in the shock-wave background, see Fig. 6 below).

The NLO impact factor for two Z^2 currents is given by the diagrams shown in Fig. 6. The gluon propagator in the shock-wave background at $x_*>0>y_*$ in the light-like gauge $p_2^\mu A_\mu=0$ is given by Eq. (43) To calculate the next-to-leading impact factor we also need the three-point scalar-scalar-gluon vertex Green function (vertex with tails) which is proportional to

$$\int d^4z\;\Big[\frac{1}{(x-z)^2}\;\overleftrightarrow{\partial_\mu}\;\frac{1}{(z-y)^2}\Big]\frac{z_\nu}{z^4}-\mu\leftrightarrow\nu \;=\; 4i\pi^2\frac{x_\mu y_\nu-x_\nu y_\mu}{x^2y^2(x-y)^2} \tag{62}$$

Using this formula, one obtains the contribution of Fig. 6a,b diagrams in the form (the details of the calculation are presented in Ref. [14])

$$\langle T\{\hat{\mathcal{O}}(x)\hat{\mathcal{O}}^\dagger(y)\}\rangle^{\rm Fig.6a,b} \;=\; \frac{\alpha_s}{(N_c^2-1)\pi^4x_*^2y_*^2}\int\frac{d^2z_1d^2z_2}{\mathcal{Z}_1^2\mathcal{Z}_2^2}\int d^2z_3\frac{z_{12}^2}{z_{13}^2z_{23}^2}{\rm Tr}\{T^nU_{z_1}U^\dagger_{z_3}T^nU_{z_3}U^\dagger_{z_2}\}\int_0^\infty\frac{d\alpha}{\alpha}\;e^{i\alpha\frac{s}{4}\mathcal{Z}_3} \tag{63}$$

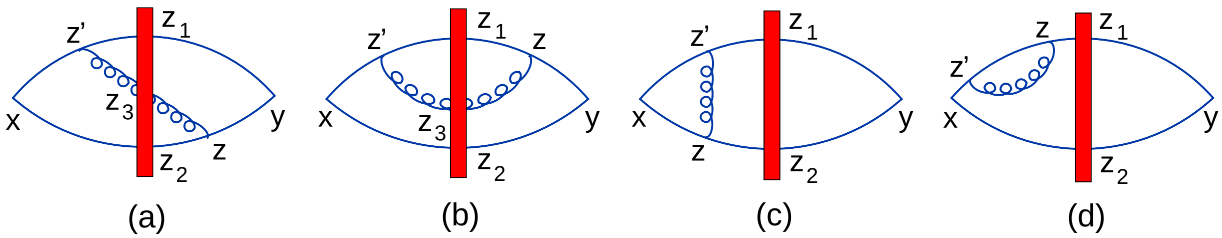

FIG. 6: Diagrams for the NLO impact factor.

Let us discuss now the contribution of Fig. 6c,d diagrams. Since this contribution is proportional to $\mathrm{Tr}\{U_{z_1}U^\dagger_{z_2}\}$ it can be restored from the comparison of Eq. (63) with the pure perturbative series for the correlator $\langle T\{\hat{\mathcal{O}}(x)\hat{\mathcal{O}}(y)\}\rangle$. If we switch off the shock wave the contribution of the Fig. 6 diagrams is given by the second term in Eq. (63) (with $U, U^\dagger$ repaced by 1). On the other hand, perturbative series for the correlator $\langle T\{\hat{\mathcal{O}}(x)\hat{\mathcal{O}}(y)\}\rangle$ vanishes [34] and therefore the contribution of the Fig. 6c,d diagrams should be equal to the second term in the r.h.s. Eq. (63) with opposite sign. Thus, we get

$$\langle T\{\hat{\mathcal{O}}(x)\hat{\mathcal{O}}^\dagger(y)\}\rangle_A^{\mathrm{Fig.6}}$$
$$= \frac{\alpha_s}{(N_c^2-1)\pi^4 x_*^2 y_*^2}\int\frac{d^2z_1d^2z_2}{\mathcal{Z}_1^2\mathcal{Z}_2^2}\int d^2z_3\frac{z_{12}^2}{z_{13}^2z_{23}^2}\Big[\mathrm{Tr}\{T^nU_{z_1}U^\dagger_{z_3}T^nU_{z_3}U^\dagger_{z_2}\}-N_c\mathrm{Tr}\{U_{z_1}U^\dagger_{z_2}\}\Big]\int_0^\infty\frac{d\alpha}{\alpha}\,e^{i\alpha\frac{s}{4}\mathcal{Z}_3} \tag{64}$$

The integral over α in the r.h.s. of Eq. (64) diverges. This divergence reflects the fact that the r.h.s. of Eq. (64) is not exactly the NLO impact factor since we must subtract the matrix element of the leading-order contribution. Indeed, the NLO impact factor is a coefficient function defined according to Eq. (61). To find the NLO impact factor, we consider the operator equation (61) in the shock-wave background (in the leading order $\langle\hat{U}_{z_3}\rangle_A = U_{z_3}$):

$$\langle T\{\hat{\mathcal{O}}(x)\hat{\mathcal{O}}(y)\}\rangle_A\ -\int d^2z_1d^2z_2\ I^{\mathrm{LO}}(x,y;z_1,z_2)\langle\mathrm{Tr}\{\hat{U}^Y_{z_1}\hat{U}^{\dagger Y}_{z_2}\}\rangle_A$$
$$= \int d^2z_1d^2z_2d^2z_3\ I^{\mathrm{NLO}}(x,y;z_1,z_2,z_3;Y)[\mathrm{Tr}\{T^nU_{z_1}U^\dagger_{z_3}T^nU_{z_3}U^\dagger_{z_2}\}-N_c\mathrm{Tr}\{U_{z_1}U^\dagger_{z_2}\}] \tag{65}$$

The NLO matrix element $\langle T\{\hat{\mathcal{O}}(x)\hat{\mathcal{O}}(y)\}\rangle_A$ is given by Eq. (64) while

$$\int d^2z_1d^2z_2\ I^{\mathrm{LO}}(x,y;z_1,z_2)\langle\mathrm{Tr}\{\hat{U}^Y_{z_1}\hat{U}^{\dagger Y}_{z_2}\}\rangle_A$$
$$= \frac{(x_*y_*)^{-2}}{\pi^2(N_c^2-1)}\int d^2z_1d^2z_2\ \frac{1}{\mathcal{Z}_1^2\mathcal{Z}_2^2}\frac{\alpha_s}{\pi^2}\int_0^\sigma\frac{d\alpha}{\alpha}\int d^2z_3\frac{z_{12}^2}{z_{13}^2z_{23}^2}[\mathrm{Tr}\{T^nU_{z_1}U^\dagger_{z_3}T^nU_{z_3}U^\dagger_{z_2}\}-N_c\mathrm{Tr}\{U_{z_1}U^\dagger_{z_2}\}] \tag{66}$$

as follows from Eqs. (32) and (48). The α integration is cut from above by $\sigma = e^Y$ in accordance with the definition of operators $\hat{U}^Y$ (30). Subtracting (66) from Eq. (64) we get

$$I^{\mathrm{NLO}}(x,y;z_1,z_2,z_3;Y) = \frac{\alpha_s(x_*y_*)^{-2}}{\pi^4(N_c^2-1)}\frac{z_{13}^2}{z_{12}^2z_{23}^2\mathcal{Z}_1^2\mathcal{Z}_2^2}\Big[\int_0^\infty\frac{d\alpha}{\alpha}\ e^{i\alpha\frac{s}{4}\mathcal{Z}_3}-\int_0^\sigma\frac{d\alpha}{\alpha}\Big]$$
$$= -\frac{\alpha_s(x_*y_*)^{-2}}{\pi^4(N_c^2-1)}\frac{z_{13}^2}{z_{12}^2z_{23}^2\mathcal{Z}_1^2\mathcal{Z}_2^2}\Big[\ln\frac{\sigma s}{4}\mathcal{Z}_3-\frac{i\pi}{2}+C\Big] \tag{67}$$

Let us rewrite the operator expansion (61) in the explicit form [14]:

$$(x-y)^4T\{\hat{\mathcal{O}}(x)\hat{\mathcal{O}}^\dagger(y)\} = \frac{1}{\pi^2(N_c^2-1)}\int\frac{d^2z_1d^2z_2}{z_{12}^4}\ \mathcal{R}^2\ \Big[\mathrm{Tr}\{\hat{U}^\sigma_{z_1}\hat{U}^{\dagger\sigma}_{z_2}\} \tag{68}$$
$$-\frac{\alpha_s}{\pi^2}\int d^2z_3\ \frac{z_{12}^2}{z_{13}^2z_{23}^2}\Big[\ln\frac{s}{4}\sigma\mathcal{Z}_3-\frac{i\pi}{2}+C\Big][\mathrm{Tr}\{T^n\hat{U}^\sigma_{z_1}\hat{U}^{\dagger\sigma}_{z_3}T^n\hat{U}^\sigma_{z_3}\hat{U}^{\dagger\sigma}_{z_2}\}-N_c\mathrm{Tr}\{\hat{U}^\sigma_{z_1}\hat{U}^{\dagger\sigma}_{z_2}\}]$$

Note that the l.h.s. of the Eq. (68) is conformally invariant while the coefficient function in the r.h.s. is not (due to $[\ln\frac{s}{4}\sigma\mathcal{Z}_3$ factor). The reason for that is the cutoff in the longitudinal direction (30). Indeed, we consider the light-like

dipoles (in the p_1 direction) and impose the cutoff on the maximal α emitted by any gluon from the Wilson lines. Formally, the light-like Wilson lines are Möbius invariant. However, the light-like Wilson lines are divergent in the longitudinal direction and moreover, it is exactly the evolution equation with respect to this longitudinal cutoff which governs the high-energy behavior of amplitudes. At present, it is not known how to find the conformally invariant cutoff in the longitudinal direction. When we use the non-invariant cutoff we expect, as usual, the invariance to hold in the leading order but be violated in higher orders in perturbation theory. In our calculation we restrict the longitudinal momentum of the gluons composing Wilson lines, and with this non-invariant cutoff the NLO evolution equation in QCD has extra non-conformal parts not related to the running of coupling constant. Similarly, there will be non-conformal parts coming from the longitudinal cutoff of Wilson lines in the $\mathcal{N} = 4$ SYM equation. We will demonstrate below that it is possible to construct the "composite conformal dipole operator" (order by order in perturbation theory) which mimics the conformal cutoff in the longitudinal direction so the corresponding evolution equation has no extra non-conformal parts. This is similar to the construction of the composite renormalized local operator in the case when the UV cutoff does not respect the symmetries of the bare operator - in this case the symmetry of the UV-regularized operator is preserved order by order in perturbation theory by subtraction of the symmetry-restoring counterterms. Following Ref. [14] we choose the conformal composite operator in the form (11)

$$\begin{aligned}&[\mathrm{Tr}\{\hat{U}_{z_1}\hat{U}^\dagger_{z_2}\}]^{\mathrm{conf}}_{a,Y}\\ &= \mathrm{Tr}\{\hat{U}^\sigma_{z_1}\hat{U}^{\dagger\sigma}_{z_2}\} + \frac{\alpha_s}{2\pi^2}\int d^2z_3\,\frac{z_{12}^2}{z_{13}^2z_{23}^2}[\mathrm{Tr}\{T^n\hat{U}^\sigma_{z_1}\hat{U}^{\dagger\sigma}_{z_3}T^n\hat{U}^\sigma_{z_3}\hat{U}^{\dagger\sigma}_{z_2}\} - N_c\mathrm{Tr}\{\hat{U}^\sigma_{z_1}\hat{U}^{\dagger\sigma}_{z_2}\}]\ln\frac{4az_{12}^2}{sz_{13}^2z_{23}^2} \;+\; O(\alpha_s^2)\end{aligned}$$

where a is an arbitrary constant. It is convenient to choose the rapidity-dependent constant $a \to ae^{-2Y}$ so that the $[\mathrm{Tr}\{\hat{U}^\sigma_{z_1}\hat{U}^{\dagger\sigma}_{z_2}\}]^{\mathrm{conf}}_a$ does not depend on $Y = \ln\sigma$ and all the rapidity dependence is encoded into a-dependence:

$$\begin{aligned}&[\mathrm{Tr}\{\hat{U}_{z_1}\hat{U}^\dagger_{z_2}\}]^{\mathrm{conf}}_{a}\\ &= \mathrm{Tr}\{\hat{U}^\sigma_{z_1}\hat{U}^{\dagger\sigma}_{z_2}\} + \frac{\alpha_s}{2\pi^2}\int d^2z_3\,\frac{z_{12}^2}{z_{13}^2z_{23}^2}[\mathrm{Tr}\{T^n\hat{U}^\sigma_{z_1}\hat{U}^{\dagger\sigma}_{z_3}T^n\hat{U}^\sigma_{z_3}\hat{U}^{\dagger\sigma}_{z_2}\} - N_c\mathrm{Tr}\{\hat{U}^\sigma_{z_1}\hat{U}^{\dagger\sigma}_{z_2}\}]\ln\frac{4az_{12}^2}{\sigma^2sz_{13}^2z_{23}^2} \;+\; O(\alpha_s^2)\end{aligned} \tag{69}$$

Using the leading-order evolution equation (48) it is easy to see that $\frac{d}{dY}[\mathrm{Tr}\{\hat{U}_{z_1}\hat{U}^\dagger_{z_2}\}]^{\mathrm{conf}}_a = 0$ (with our $O(\alpha_s^2)$ accuracy).

Rewritten in terms of conformal dipoles (69), the operator expansion (68) takes the form:

$$\begin{aligned}(x-y)^4T\{\hat{\mathcal{O}}(x)\hat{\mathcal{O}}^\dagger(y)\} \;&=\; \frac{1}{\pi^2(N_c^2-1)}\int\frac{d^2z_1d^2z_2}{z_{12}^4}\;\mathcal{R}^2\;\Big\{[\mathrm{Tr}\{\hat{U}_{z_1}\hat{U}^\dagger_{z_2}\}]^{\mathrm{conf}}_a\\ &- \frac{\alpha_s}{2\pi^2}\int d^2z_3\frac{z_{12}^2}{z_{13}^2z_{23}^2}\Big(\ln\frac{asz_{12}^2}{4z_{13}^2z_{23}^2}\mathcal{Z}_3^2 - i\pi + 2C\Big)[\mathrm{Tr}\{T^n\hat{U}_{z_1}\hat{U}^\dagger_{z_3}T^n\hat{U}_{z_3}\hat{U}^\dagger_{z_2}\} - N_c\mathrm{Tr}\{\hat{U}_{z_1}\hat{U}^\dagger_{z_2}\}]_a\Big\}\end{aligned} \tag{70}$$

We need to choose the new "rapidity cutoff" a in such a way that all the energy dependence is included in the matrix element(s) of Wilson-line operators so the impact factor should not depend on energy ($\equiv$ should not scale with ρ as $\rho \to \infty$). A suitable choice of a is given by $a_0 = \kappa^{-2} + i\epsilon = \frac{4x_*y_*}{s(x-y)^2} + i\epsilon$ so we obtain

$$\begin{aligned}(x-y)^4T\{\hat{\mathcal{O}}(x)\hat{\mathcal{O}}^\dagger(y)\} \;&=\; \frac{1}{\pi^2(N_c^2-1)}\int\frac{d^2z_1d^2z_2}{z_{12}^4}\;\mathcal{R}^2\;\Big\{[\mathrm{Tr}\{\hat{U}^\sigma_{z_1}\hat{U}^{\dagger\sigma}_{z_2}\}]^{\mathrm{conf}}_{a_0}\\ &- \frac{\alpha_s}{2\pi^2}\int d^2z_3\frac{z_{12}^2}{z_{13}^2z_{23}^2}\Big[\ln\frac{-x_*y_*z_{12}^2}{(x-y)^2z_{13}^2z_{23}^2}\mathcal{Z}_3^2 + 2C\Big][\mathrm{Tr}\{T^n\hat{U}^\sigma_{z_1}\hat{U}^{\dagger\sigma}_{z_3}T^n\hat{U}^\sigma_{z_3}\hat{U}^{\dagger\sigma}_{z_2}\} - N_c\mathrm{Tr}\{\hat{U}^\sigma_{z_1}\hat{U}^{\dagger\sigma}_{z_2}\}]\Big\}\end{aligned} \tag{71}$$

where the conformal dipole $[\mathrm{Tr}\{\hat{U}^\sigma_{z_1}\hat{U}^{\dagger\sigma}_{z_2}\}]^{\mathrm{conf}}$ is given by Eq. (69) with $a_0 = \frac{4x_*y_*}{s(x-y)^2}$.

Now it is evident that the impact factor in the r.h.s. of this equation is Möbius invariant and does not scale with ρ so Eq. (69) gives conformally invariant operator up to α_s^2 order. In higher orders, one should expect the correction terms with more Wilson lines.

With the two-gluon accuracy integration over one z in the r.h.s. of Eq. (71) can be performed explicitly so that the resulting operator expansion takes the form

$$\begin{aligned}&(x-y)^4T\{\hat{\mathcal{O}}(x)\hat{\mathcal{O}}^\dagger(y)\}\\ &= -\frac{1}{\pi^2}\int\frac{dz_1dz_2}{z_{12}^4}\;\hat{\mathcal{U}}^{a_0}_{\mathrm{conf}}(z_1,z_2)\mathcal{R}^2\Big\{1 - \frac{\alpha_sN_c}{2\pi}\Big[\ln^2\mathcal{R} - \frac{\ln\mathcal{R}}{\mathcal{R}} - 2C\big(\ln\mathcal{R} - \frac{1}{\mathcal{R}} + 2\big) + 2\mathrm{Li}_2(1-\mathcal{R}) - \frac{\pi^2}{3}\Big]\Big\}\end{aligned} \tag{72}$$

We need the projection of the T-product in the l.h.s. of this equation onto the conformal eigenfunctions of the BFKL equation with spin 0 (cf. Eq. (36)

$$\begin{aligned}&\frac{1}{\pi^2}\int\frac{dz_1dz_2}{z_{12}^4}\,\mathcal{R}^2\Big\{1-\frac{\alpha_sN_c}{2\pi}\Big[\ln^2\mathcal{R}-\frac{\ln\mathcal{R}}{\mathcal{R}}-2C\big(\ln\mathcal{R}-\frac{1}{\mathcal{R}}+2\big)+\ 2\mathrm{Li}_2(1-\mathcal{R})-\frac{\pi^2}{3}\Big]\Big\}\Big[\frac{z_{12}^2}{z_{10}^2z_{20}^2}\Big]^{\frac12+i\nu}\\ &=\ \Big[\frac{-\kappa^2}{(-2\kappa\cdot\zeta_0)^2}\Big]^{\frac12+i\nu}\frac{\Gamma^2\big(\frac12-i\nu\big)}{\Gamma(1-2i\nu)}\frac{\big(\frac14+\nu^2\big)\pi}{\cosh\pi\nu}\Big\{1+\frac{\alpha_sN_c}{2\pi}\Phi_1(\nu)\Big\}\end{aligned}\tag{73}$$

where

$$\Phi_1(\nu)\ =\ -2\psi'\big(\frac12+i\nu\big)-2\psi'\big(\frac12-i\nu\big)+\frac{2\pi^2}{3}+\frac{\chi(\nu)-2}{\nu^2+\frac14}+2C\chi(\nu)\tag{74}$$

and $\zeta_0\equiv\frac{p_1}{s}+z_{0\perp}^2p_2+z_{0\perp}$.

Now, using the decomposition (37) of the product of the transverse δ-functions in conformal 3-point functions $E_{\nu,n}(z_{10},z_{20})$ we obtain

$$\begin{aligned}&(x-y)^4T\{\hat{\mathcal{O}}(x)\hat{\mathcal{O}}^\dagger(y)\}\\ &=\ -\int d\nu\int d^2z_0\ \frac{\nu^2(1+4\nu^2)}{4\pi\cosh\pi\nu}\frac{\Gamma^2\big(\frac12-i\nu\big)}{\Gamma(1-2i\nu)}\ \Big(\frac{-\kappa^2}{(-2\kappa\cdot\zeta_0)^2}\Big)^{\frac12+i\nu}\big[1+\frac{\alpha_sN_c}{2\pi}\Phi_1(\nu)\big]\hat{\mathcal{U}}^a_{\rm conf}(\nu,z_0)\end{aligned}\tag{75}$$

where

$$\hat{\mathcal{U}}^a_{\rm conf}(\nu,z_0)\ \equiv\ \frac{1}{\pi^2}\int\frac{d^2z_1d^2z_2}{z_{12}^4}\ \Big(\frac{z_{12}^2}{z_{10}^2z_{20}^2}\Big)^{\frac12-i\nu}\ \hat{\mathcal{U}}^a_{\rm conf}(z_1,z_2)\tag{76}$$

is a conformal dipole in the z_0,ν representation.

D. NLO BK in $\mathcal{N}=4$ SYM

The typical diagrams for the NLO evolution of color dipole are shown Fig. 7. Here solid line depicts either scalar particle or gluino. The contribution of these diagrams is calculated using the gluon propagator in a shock-

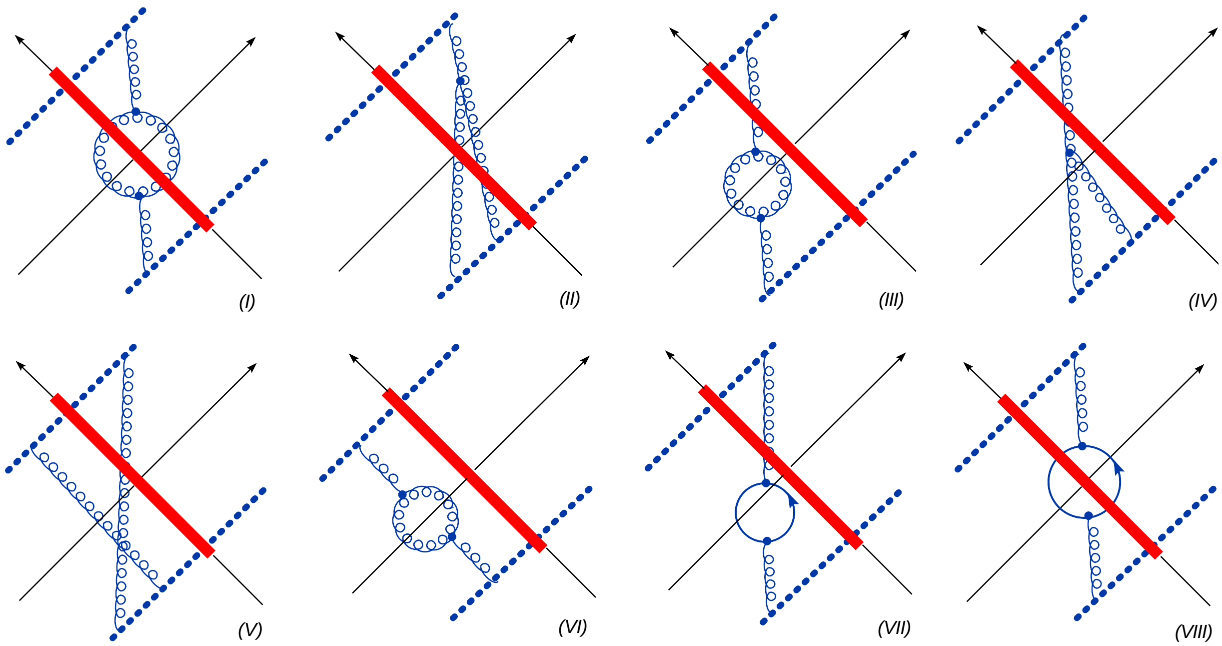

FIG. 7: Different types of diagrams for the NLO evolution of color dipole.

wave background (43) and usual Yang-Mills vertices. The typical contribution has a form of an integral over Feynman parameter which is a fraction of momentum α carried by one of the gluon after splitting described by the three- gluon vertex. For example,

$$\begin{aligned}\langle \mathrm{Tr}\{\hat U_x \hat U^\dagger_y\}\rangle_{\mathrm{Fig.7I}} &= \frac{\alpha_s^2}{8\pi^4}\ln\Delta Y\int_0^1 du\ u\bar u\int d^2z d^2z'\ U_z^{bb'}U_{z'}^{cc'}\\ &\times \mathrm{Tr}\Big\{T^a f^{abc}\Big[\frac{Z_{ij}}{(z-z')^2[uz_{13}^2+\bar u z_{14}^2]}-(z_1\leftrightarrow z_2)\Big]\Big\}U_x\Big\{T^{a'}f^{a'b'c'}\Big[\frac{Z'_{ij}}{(z-z')^2[uz_{23}^2+\bar u z_{24}^2]}-(z_1\leftrightarrow z_2)\Big]\Big\}U_y^\dagger \end{aligned}\quad (77)$$

where

$$Z^{ij} = (z_{13}^2-z_{14}^2)g^{ij}+\frac{2}{u}z_{34}^i z_{14}^j+\frac{2}{\bar u}z_{13}^i z_{34}^j, \qquad Z'^{ij} = (z_{23}^2-z_{24}^2)g^{ij}+\frac{2}{u}z_{34}^i z_{24}^j+\frac{2}{\bar u}z_{23}^i z_{34}^j \quad (78)$$

and $\bar u \equiv 1-u$. It is easy to see that integral (77) diverges as $u\to 0$ and $u\to 1$. This divergence comes in the momentum space from the integrals of the type

$$\int_0^\infty d\alpha_1 d\alpha_2\ \frac{1}{\alpha_1(k_{1\perp}^2\alpha_2+k_{1\perp}^2\alpha_2)}$$

where $\alpha_i p_1$ and $k_{i\perp}$ are longitudinal and transverse momenta carried by gluons in the loop in Fig. 7I. If we put a lower cutoff $\alpha_i>\sigma'$ on the α_i integrals we would get a contribution $\sim\ln^2\frac{\sigma}{\sigma'}$ coming from the region $\alpha_2\gg\alpha_1>\sigma'$ (or $\alpha_1\gg\alpha_2>\sigma'$) which corresponds to the the square of the leading-order BK kernel rather than to the NLO kernel. To get the NLO kernel we need to subtract this $(LO)^2$ contribution. Indeed, the operator form of the evolution equation for the color dipole up to the next-to-leading order looks like

$$\frac{d}{dY}\mathrm{Tr}\{\hat U_x\hat U^\dagger_y\} = K_{\mathrm{LO}}\mathrm{Tr}\{\hat U_x\hat U^\dagger_y\}+K_{\mathrm{NLO}}\mathrm{Tr}\{\hat U_x\hat U^\dagger_y\} \quad (79)$$

where $Y=\ln\sigma$. Our goal is to find K_{NLO} by considering the l.h.s. of this equation in the external shock-wave background so

$$\langle K_{\mathrm{NLO}}\mathrm{Tr}\{\hat U_x\hat U^\dagger_y\}\rangle_{\mathrm{shockwave}} = \frac{d}{dY}\langle \mathrm{Tr}\{\hat U_x\hat U^\dagger_y\}\rangle_{\mathrm{shockwave}} - \langle K_{\mathrm{LO}}\mathrm{Tr}\{\hat U_x\hat U^\dagger_y\}\rangle_{\mathrm{shockwave}} \quad (80)$$

The subtraction (80) leads to the $\left[\frac{1}{u}\right]_+$ prescription (14) for the terms divergent as $\frac{1}{u}$ (similarly, $\frac{1}{\bar u}\to\left[\frac{1}{\bar u}\right]_+$ for the contribution divergent as $u\to 1$). With this prescription, the integrals over the Feynman parameter converge. The

calculation of diagrams is carried out in Refs. [14, 19] and the result has the form

$$\frac{d}{dY}\mathrm{Tr}\{\hat U^Y_{z_1}\hat U^{\dagger Y}_{z_2}\} = \frac{\alpha_s}{\pi^2}\int d^2z_3~\frac{z_{12}^2}{z_{13}^2z_{23}^2}\Big\{1-\frac{\alpha_sN_c}{4\pi}\Big[\frac{\pi^2}{3}+2\ln\frac{z_{13}^2}{z_{12}^2}\ln\frac{z_{23}^2}{z_{12}^2}\Big]\Big\}[\mathrm{Tr}\{T^a\hat U^Y_{z_1}\hat U^{\dagger Y}_{z_3}T^a\hat U^Y_{z_3}\hat U^{\dagger Y}_{z_2}\}-N_c\mathrm{Tr}\{\hat U^Y_{z_1}\hat U^{\dagger Y}_{z_2}\}]$$
$$-\frac{\alpha_s^2}{4\pi^4}\int\frac{d^2z_3d^2z_4}{z_{34}^4}~\frac{z_{12}^2z_{34}^2}{z_{13}^2z_{24}^2}\Big[1+\frac{z_{12}^2z_{34}^2}{z_{13}^2z_{24}^2-z_{23}^2z_{14}^2}\Big]\ln\frac{z_{13}^2z_{24}^2}{z_{14}^2z_{23}^2}$$
$$\times~\mathrm{Tr}\{[T^a,T^b]\hat U^Y_{z_1}T^{a'}T^{b'}\hat U^{\dagger Y}_{z_2}+T^bT^a\hat U^Y_{z_1}[T^{b'},T^{a'}]\hat U^{\dagger Y}_{z_2}\}(\hat U^Y_{z_3})^{aa'}(\hat U^Y_{z_4}-\hat U^Y_{z_3})^{bb'}. \tag{81}$$

All terms in the r.h.s. of this equation are Möbius invariant except the double-log term proportional to $\ln\frac{z_{13}^2}{z_{12}^2}\ln\frac{z_{23}^2}{z_{12}^2}$. As was discussed in the Introduction, the reason for this non-invariance is the cutoff in the longitudinal direction which violates the formal invariance of the non-cut Wilson lines.

It is worth noting that conformal and non-conformal terms come from graphs with different topology: the conformal terms come from 1→3 dipoles diagrams (see Fig. 6 in Ref. [19]) which describe the dipole creation while the non-conformal double-log term comes from the 1→2 dipole transitions (Fig.9 in Ref. [19])) which can be regarded as a combination of dipole creation and dipole recombination.

Our aim is to rewrite the evolution equation in terms of composite conformal dipoles (69). In the next-to-leading order the conformal dipole has the form

$$\big[\mathrm{Tr}\{\hat U_{z_1}\hat U^\dagger_{z_2}\}\big]^{\rm conf}_a = \mathrm{Tr}\{\hat U^Y_{z_1}\hat U^{\dagger Y}_{z_2}\} \tag{82}$$
$$+\frac{\alpha_s}{2\pi^2}\int d^2z_3~\frac{z_{12}^2}{z_{13}^2z_{23}^2}\Big[1-\frac{\alpha_sN_c}{4\pi}\frac{\pi^2}{3}\Big]\big[\mathrm{Tr}\{T^a\hat U^Y_{z_1}\hat U^{\dagger Y}_{z_3}T^a\hat U^Y_{z_3}\hat U^{\dagger Y}_{z_2}\}-N_c\mathrm{Tr}\{\hat U^Y_{z_1}\hat U^{\dagger Y}_{z_2}\}\big]\ln\frac{4az_{12}^2}{\sigma^2sz_{13}^2z_{23}^2}$$
$$-\frac{\alpha_s^2}{8\pi^4}\int d^2z_3d^2z_4\frac{z_{12}^2}{z_{13}^2z_{24}^2z_{34}^2}\Big\{2\ln\frac{z_{12}^2z_{34}^2}{z_{14}^2z_{23}^2}+\Big[1+\frac{z_{12}^2z_{34}^2}{z_{13}^2z_{24}^2-z_{14}^2z_{23}^2}\Big]\ln\frac{z_{13}^2z_{24}^2}{z_{14}^2z_{23}^2}\Big\}\ln\frac{4a}{\sigma^2s}f(z_i)$$
$$\times~\mathrm{Tr}\{[T^a,T^b]\hat U^Y_{z_1}T^{a'}T^{b'}\hat U^{\dagger Y}_{z_2}+T^bT^a\hat U^Y_{z_1}[T^{b'},T^{a'}]\hat U^{\dagger Y}_{z_2}\}[(\hat U^Y_{z_3})^{aa'}(\hat U^Y_{z_4})^{bb'}-(z_4\to z_3)]$$
$$+\frac{\alpha_s}{32\pi^4}\int d^2z_3~\frac{z_{12}^2}{z_{13}^2z_{23}^2}\int d^2z_4(\hat U^Y_{z_3})^{aa'}$$
$$\times\Big\{\mathrm{Tr}\{T^aT^b\hat U^Y_{z_1}T^{a'}T^{b'}\hat U^{\dagger Y}_{z_2}+T^bT^a\hat U^Y_{z_1}T^{b'}T^{a'}\hat U^{\dagger Y}_{z_2}\}(2\hat U^Y_{z_4}-\hat U^Y_{z_1}-\hat U^Y_{z_2})^{bb'}\frac{z_{12}^2}{z_{14}^2z_{24}^2}\ln^2\big(\frac{az_{12}^2}{\sigma^2sz_{14}^2z_{24}^2}\big)$$
$$-~\mathrm{Tr}\{T^aT^b\hat U^Y_{z_1}[T^{a'},T^{b'}]\hat U^{\dagger Y}_{z_2}+[T^b,T^a]\hat U^Y_{z_1}T^{b'}T^{a'}\hat U^{\dagger Y}_{z_2}\}(2\hat U^Y_{z_4}-\hat U^Y_{z_1}-\hat U^Y_{z_3})^{bb'}\frac{z_{13}^2}{z_{14}^2z_{34}^2}\ln^2\big(\frac{4az_{13}^2}{\sigma^2sz_{14}^2z_{34}^2}\big)$$
$$-~\mathrm{Tr}\{[T^a,T^b]\hat U^Y_{z_1}T^{a'}T^{b'}\hat U^{\dagger Y}_{z_2}+T^bT^a\hat U^Y_{z_1}[T^{b'},T^{a'}]\hat U^{\dagger Y}_{z_2}\}(2\hat U^Y_{z_4}-\hat U^Y_{z_2}-\hat U^Y_{z_3})^{bb'}\frac{z_{23}^2}{z_{24}^2z_{34}^2}\ln^2\big(\frac{4az_{23}^2}{\sigma^2sz_{24}^2z_{34}^2}\big)\Big\}$$
$$-\frac{\alpha_s^2N_c}{8\pi^4}\int d^2z_3~\frac{z_{12}^2}{z_{13}^2z_{23}^2}\int d^2z_4\frac{z_{12}^2}{z_{14}^2z_{24}^2}(\mathrm{Tr}\{T^aU_{z_1}U^\dagger_{z_4}T^aU_{z_4}U^\dagger_{z_2}\}-N_c\mathrm{Tr}\{U_{z_1}U^\dagger_{z_2}\})\ln^2\big(\frac{4az_{12}^2}{\sigma^2sz_{14}^2z_{24}^2}\big)$$

where function f is undetermined in the NLO (to fix it one needs the NNLO accuracy). Using the equations for $\frac{d}{dY}\mathrm{Tr}\{\hat U^Y_{z_1}\hat U^{\dagger Y}_{z_2}\}$ and $\frac{d}{dY}\big[\mathrm{Tr}\{T^a\hat U^Y_{z_1}\hat U^{\dagger Y}_{z_3}T^a\hat U_{z_3}\hat U^{\dagger Y}_{z_2}\}-N_c\mathrm{Tr}\{\hat U^Y_{z_1}\hat U^{\dagger Y}_{z_2}\}\big]$ from Ref. [14] one can demonstrate that $\frac{d}{dY}\big[\mathrm{Tr}\{\hat U_{z_1}\hat U^\dagger_{z_2}\}\big]^{\rm conf}_a = 0$.

Differentiating now with respect to a we get

$$2a\frac{d}{da}\big[\mathrm{Tr}\{\hat U_{z_1}\hat U^\dagger_{z_2}\}\big]^{\rm conf}_a = \frac{\alpha_s}{\pi^2}\int d^2z_3~\frac{z_{12}^2}{z_{13}^2z_{23}^2}\Big[1-\frac{\alpha_sN_c}{4\pi}\frac{\pi^2}{3}\Big]\big[\mathrm{Tr}\{T^a\hat U_{z_1}\hat U^\dagger_{z_3}T^a\hat U_{z_3}\hat U^\dagger_{z_2}\}-N_c\mathrm{Tr}\{\hat U_{z_1}\hat U^\dagger_{z_2}\}\big]^{\rm conf}_a$$
$$-\frac{\alpha_s^2}{4\pi^4}\int d^2z_3d^2z_4\frac{z_{12}^2}{z_{13}^2z_{24}^2z_{34}^2}\Big\{2\ln\frac{z_{12}^2z_{34}^2}{z_{14}^2z_{23}^2}+\Big[1+\frac{z_{12}^2z_{34}^2}{z_{13}^2z_{24}^2-z_{14}^2z_{23}^2}\Big]\ln\frac{z_{13}^2z_{24}^2}{z_{14}^2z_{23}^2}\Big\}$$
$$\times~\mathrm{Tr}\{[T^a,T^b]\hat U_{z_1}T^{a'}T^{b'}\hat U^\dagger_{z_2}+T^bT^a\hat U_{z_1}[T^{b'},T^{a'}]\hat U^\dagger_{z_2}\}[(\hat U_{z_3})^{aa'}(\hat U_{z_4})^{bb'}-(z_4\to z_3)] \tag{83}$$

where

$$[\mathrm{Tr}\{T^a\hat U_{z_1}\hat U^\dagger_{z_3}T^a\hat U_{z_3}\hat U^\dagger_{z_2}\}-N_c\mathrm{Tr}\{\hat U_{z_1}\hat U^\dagger_{z_2}\}]^{\rm conf}_a\ =\ \mathrm{Tr}\{T^a\hat U^Y_{z_1}\hat U^{\dagger Y}_{z_3}T^a\hat U^Y_{z_3}\hat U^{\dagger Y}_{z_2}\}-N_c\mathrm{Tr}\{\hat U^Y_{z_1}\hat U^{\dagger Y}_{z_2}\}$$
$$+\ \frac{\alpha_s}{8\pi^2}\int d^2z_4(\hat U^Y_{z_3})^{aa'}\Big[\mathrm{Tr}\{T^aT^b\hat U^Y_{z_1}T^{a'}T^{b'}\hat U^{\dagger Y}_{z_2}+T^bT^a\hat U^Y_{z_1}T^{b'}T^{a'}\hat U^{\dagger Y}_{z_2}\}(2\hat U^Y_{z_4}-\hat U^Y_{z_1}-\hat U^Y_{z_2})^{bb'}\frac{z^2_{12}}{z^2_{14}z^2_{24}}\ln\frac{4az^2_{12}}{s\sigma^2z^2_{14}z^2_{24}}$$
$$-\ \mathrm{Tr}\{T^aT^b\hat U^Y_{z_1}[T^{a'},T^{b'}]\hat U^{\dagger Y}_{z_2}+[T^b,T^a]\hat U^Y_{z_1}T^{b'}T^{a'}\hat U^{\dagger Y}_{z_2}\}(2\hat U^Y_{z_4}-\hat U^Y_{z_1}-\hat U^Y_{z_3})^{bb'}\frac{z^2_{13}}{z^2_{14}z^2_{34}}\ln\frac{4az^2_{13}}{s\sigma^2z^2_{14}z^2_{34}}$$
$$-\ \mathrm{Tr}\{[T^a,T^b]\hat U^Y_{z_1}T^{a'}T^{b'}\hat U^{\dagger Y}_{z_2}+T^bT^a\hat U^Y_{z_1}[T^{b'},T^{a'}]\hat U^{\dagger Y}_{z_2}\}(2\hat U^Y_{z_4}-\hat U^Y_{z_2}-\hat U^Y_{z_3})^{bb'}\frac{z^2_{23}}{z^2_{24}z^2_{34}}\ln\frac{4az^2_{23}}{s\sigma^2z^2_{24}z^2_{34}}\Big]$$
$$-\ \frac{\alpha_sN_c}{2\pi^2}\int d^2z_4\frac{z^2_{12}}{z^2_{14}z^2_{24}}(\mathrm{Tr}\{T^aU_{z_1}U^\dagger_{z_4}T^aU_{z_4}U^\dagger_{z_2}\}-N_c\mathrm{Tr}\{U_{z_1}U^\dagger_{z_2}\})\ln\frac{4az^2_{12}}{s\sigma^2z^2_{14}z^2_{24}}\ +\ O(\alpha_s^2) \tag{84}$$

is a conformal Y-independent operator found in Ref. [14]. One sees now that the evolution equation with respect to parameter a (83) is obviously Möbius invariant.

E. NLO evolution of the conformal dipole

With out two-gluon accuracy the evolution equation (83) reduces to

$$2a\frac{d}{da}\hat{\mathcal U}^a_{\rm conf}(z_1,z_2)\ =\ \int d^2z_3d^2z_4[K_{\rm LO}(z_1,z_2;z_3,z_4)+K_{\rm NLO}(z_1,z_2;z_3,z_4)]\ \hat{\mathcal U}^a_{\rm conf}(z_3,z_4) \tag{85}$$

where the kernel $K_{\rm NLO}(z_1,z_2;z_3,z_4)$ in the first two orders has the form [19, 27] (see also Ref. [35])

$$K_{\rm NLO}(z_1,z_2;z_3,z_4)\ =\ -\frac{\alpha_sN_c}{4\pi}\frac{\pi^2}{3}K_{\rm LO}(z_1,z_2;z_3,z_4)$$
$$+\ \frac{\alpha_s^2N_c^2}{8\pi^4z^4_{34}}\left[\frac{z^2_{12}z^2_{34}}{z^2_{13}z^2_{24}}\Big\{\Big(1+\frac{z^2_{12}z^2_{34}}{z^2_{13}z^2_{24}-z^2_{14}z^2_{23}}\Big)\ln\frac{z^2_{13}z^2_{24}}{z^2_{14}z^2_{23}}+2\ln\frac{z^2_{12}z^2_{34}}{z^2_{14}z^2_{23}}\Big\}+12\pi^2\zeta(3)z^4_{34}\delta(z_{13})\delta(z_{24})\right] \tag{86}$$

Once we know that the kernel $K_{\rm NLO}$ is conformal, its eigenfunctions are fixed by conformal invariance (see Eq. (35)) and calculation of the eigenvalues reproduces the pomeron intercept (27).

$$\int d^2z_3d^2z_4\ K(z_1,z_2;z_3,z_4)E_{\nu,n}(z_{30},z_{40})\ =\ \omega(n,\nu)E_{\nu,n}(z_{10},z_{20}) \tag{87}$$

For the composite operators with definite conformal spin (76) the evolution equation (85) takes the simple form

$$2a\frac{d}{da}\hat{\mathcal U}^a_{\rm conf}(\nu,z_0)\ =\ \omega(\nu)\hat{\mathcal U}^a_{\rm conf}(\nu,z_0) \tag{88}$$

The result of the evolution (88) is

$$\hat{\mathcal U}^a_{\rm conf}(\nu,z_0)\ =\ (a/\tilde a)^{\frac12\omega(\nu)}\hat{\mathcal U}^{a_0}_{\rm conf}(\nu,z_0) \tag{89}$$

where the endpoint of the evolution $\tilde a$ should be taken from the requirement that the amplitude of scattering of conformal dipoles with "normalization points" $\tilde a$ and b should not contain large logarithms of energy so it will serve as the initial point of the evolution (cf. Eq. (56) for the leading order).

F. NLO scattering of conformal dipoles and the NLO amplitude

The last step of our program is the "matrix element" of the conformal dipole

$$\langle T\{\hat{\mathcal U}^{\tilde a}_{\rm conf}(\nu,z_0)\mathcal O(x')\mathcal O^\dagger(y')\}\rangle \tag{90}$$

As we have done for the leading order, we start with the high-energy OPE for $\mathcal O(x')\mathcal O^\dagger(y')$

$$(x'-y')^4T\{\hat{\mathcal O}(x')\hat{\mathcal O}^\dagger(y')\}$$
$$=\ -\int d\nu'\int d^2z'_0\ \frac{\nu'^2(1+4\nu'^2)}{4\pi\cosh\pi\nu'}\frac{\Gamma^2\big(\frac12-i\nu'\big)}{\Gamma(1-2i\nu')}\ \Big(\frac{-\kappa'^2}{(-2\kappa'\cdot\zeta'_0)^2}\Big)^{\frac12+i\nu'}[1+\frac{\alpha_sN_c}{2\pi}\Phi_1(\nu')]\hat{\mathcal V}^{b_0}_{\rm conf}(\nu',z'_0). \tag{91}$$

where $b_0 = 1/\kappa'^2$and the conformal operator $\hat{\mathcal{V}}^b_{\rm conf}(z_1, z_2)$ is given by Eq. (53).

Now we multiply Eq. (91) by the NLO amplitude of scattering of two conformal dipoles [36]:

$$\langle\hat{\mathcal{U}}^{\tilde a}_{\rm conf}(\nu,z_0)\hat{\mathcal{V}}^b_{\rm conf}(\nu',z_0')\rangle \;=\; -\frac{\alpha_s^2N_c^2}{N_c^2-1}\frac{16\pi^2}{\nu^2(1+4\nu^2)^2}\Big[\delta(z_0-z_0')\delta(\nu+\nu')$$
$$+\frac{2^{1-4i\nu}\delta(\nu-\nu')}{\pi|z_0-z_0'|^{2-4i\nu}}\frac{\Gamma\big(\frac{1}{2}+i\nu\big)\Gamma(1-i\nu)}{\Gamma(i\nu)\Gamma\big(\frac{1}{2}-i\nu\big)}\Big]\Big[1+\frac{\alpha_sN_c}{2\pi}\Big(\chi(\nu)\big[\ln\tilde ab-i\pi-4C-\frac{2}{\nu^2+\frac{1}{4}}\big]-\frac{\pi^2}{3}\Big)\Big]. \tag{92}$$

From this equation we see that we need to stop the evolution (89) at $\tilde a = 1/b$. With this choice of $\tilde a$ the correlation function takes the form:

$$\langle T\{\hat{\mathcal{U}}^{\tilde a}_{\rm conf}(\nu,z_0)\mathcal{O}(x')\mathcal{O}^\dagger(y')\}\rangle \;=\; -\frac{\alpha_s^2N_c^2}{N_c^2-1}$$
$$\times\;\frac{8\pi\Gamma^2\big(\frac{1}{2}+i\nu\big)}{(1+4\nu^2)\cosh\pi\nu\Gamma(1+2i\nu)}\;\Big(\frac{-\kappa'^2}{(-2\kappa'\cdot\zeta_0)^2}\Big)^{\frac{1}{2}+i\nu}\big[1+\frac{\alpha_sN_c}{2\pi}\Phi_1(\nu)\big]\Big[1-\frac{\alpha_sN_c}{2\pi}\Big(\chi(\nu)\big[i\pi+4C+\frac{2}{\nu^2+\frac{1}{4}}\big]+\frac{\pi^2}{3}\Big)\Big]. \tag{93}$$

Finally, substituting this amplitude in Eq. (75) we obtain Eq. (23) with

$$F(\nu) \;=\; \frac{N_c^2}{N_c^2-1}\frac{4\pi^4\alpha_s^2}{\cosh^2\pi\nu}\;\big[1+\frac{\alpha_sN_c}{2\pi}\Phi_1(\nu)\big]^2\;\Big\{1-\frac{\alpha_sN_c}{2\pi}\Big[\chi(\nu)\Big(4C+\frac{8}{1+4\nu^2}\Big)+\frac{\pi^2}{3}\Big]+O(\alpha_s^2)\Big\}$$
$$=\;\frac{N_c^2}{N_c^2-1}\frac{4\pi^4\alpha_s^2}{\cosh^2\pi\nu}\;\Big\{1+\frac{\alpha_sN_c}{\pi}\Big[-2\psi'\big(\frac{1}{2}+i\nu\big)-2\psi'\big(\frac{1}{2}-i\nu\big)+\frac{\pi^2}{2}-\frac{8}{1+4\nu^2}\Big]+O(\alpha_s^2)\Big\} \tag{94}$$

which gives the pomeron residue in the next-to-leading order.

It is instructive to represent this result in a way symmetric between projectile and target as a product of spectator impact factor, target impact factor, and scattering of two (conformal) dipoles as shown in Fig. 8.

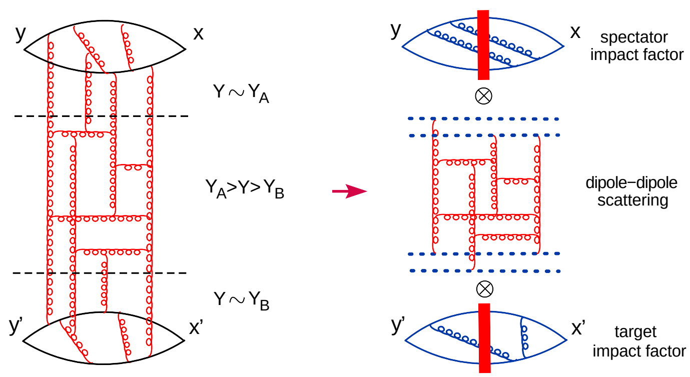

FIG. 8: High-energy factorization into the product of two impact factors and dipole-dipole scattering

Combining the operator expansions (75) and (91) we get

$$(x-y)^4(x'-y')^4\langle T\{\hat{\mathcal{O}}(x)\hat{\mathcal{O}}^\dagger(y)\hat{\mathcal{O}}(x')\hat{\mathcal{O}}^\dagger(y')\}\rangle$$
$$=\;\int d\nu d\nu'\int d^2z_0d^2z_0'\;\frac{\nu^2(1+4\nu^2)}{4\pi\cosh\pi\nu}\frac{\Gamma^2\big(\frac{1}{2}-i\nu\big)}{\Gamma(1-2i\nu)}\Big(\frac{-\kappa^2}{(-2\kappa\cdot\zeta_0)^2}\Big)^{\frac{1}{2}+i\nu}\big[1+\frac{\alpha_sN_c}{2\pi}\Phi_1(\nu)\big]$$
$$\times\;\frac{\nu'^2(1+4\nu'^2)}{4\pi\cosh\pi\nu'}\frac{\Gamma^2\big(\frac{1}{2}-i\nu'\big)}{\Gamma(1-2i\nu')}\Big(\frac{-\kappa'^2}{(-2\kappa'\cdot\zeta_0')^2}\Big)^{\frac{1}{2}+i\nu'}\big[1+\frac{\alpha_sN_c}{2\pi}\Phi_1(\nu')\big]\langle\hat{\mathcal{U}}^{a_0}_{\rm conf}(\nu,z_0)\hat{\mathcal{V}}^{b_0}_{\rm conf}(\nu',z_0')\rangle \tag{95}$$

The scattering of two conformal dipoles is obtained from Eq. (92) by evolution (89):

$$\langle\hat{\mathcal{U}}^a_{\rm conf}(\nu,z_0)\hat{\mathcal{V}}^b_{\rm conf}(\nu',z_0')\rangle$$
$$=\;i\frac{\alpha_s^2N_c^2}{N_c^2-1}\frac{(a+i\epsilon)^{\frac{\omega(\nu)}{2}}(b+i\epsilon)^{\frac{\omega(\nu)}{2}}-(-a-i\epsilon)^{\frac{\omega(\nu)}{2}}(-b-i\epsilon)^{\frac{\omega(\nu)}{2}}}{\sin\pi\omega(\nu)}\Big[1-\frac{\alpha_sN_c}{2\pi}\Big(\chi(\gamma)\big[4C+\frac{8}{1+4\nu^2}\big]+\frac{\pi^2}{3}\Big)\Big]$$
$$\times\;\frac{16\pi^2}{\nu^2(1+4\nu^2)^2}\Big[\delta(z_0-z_0')\delta(\nu+\nu')+\frac{2^{1-4i\nu}\delta(\nu-\nu')}{\pi|z_0-z_0'|^{2-4i\nu}}\frac{\Gamma\big(\frac{1}{2}+i\nu\big)\Gamma(1-i\nu)}{\Gamma(i\nu)\Gamma\big(\frac{1}{2}-i\nu\big)}\Big]. \tag{96}$$

Substituting this amplitude with $a_0 = \kappa^{-2} + i\epsilon$ and $b_0 = {\kappa'}^{-2} + i\epsilon$ in Eq. (95) we reobtain Eq. (23) with the pomeron residue (94).

V. NEXT-TO-LEADING ORDER IN QCD

In $\mathcal{N} = 4$ SYM we were able to perform all four steps of our program and arrive at explicit result (23) with $\omega(\nu)$ and $F(\nu)$ given by Eqs. (3) and (94), respectively. In QCD, we do not have conformal invariance so there is no general formula for the pomeron contribution similar to Eq. (23). Moreover, by the same reason (absence of Mobius invariance) we cannot solve the equation for evolution of color dipoles analytically. Here I will describe the first two steps of OPE program - (1) operator expansion in color dipoles and (2) evolution equation for color dipoles.

A. High-energy OPE and photon impact factor

I will consider the process of deep inelastic scattering (DIS) at small Bjorken x. As I discussed in Sect. III, the virtual photon splits in to $q\bar{q}$ pair which moves in an "external" field of target's gluons. To calculate the leading-order impact factor, we need the quark propagator in the shock-wave background. It has the form [7]

$$\begin{aligned}\langle\hat{\psi}(x)\hat{\bar{\psi}}(y)\rangle \;&=\; \theta(x_*y_*)\frac{(\not{x}-\not{y})}{2\pi^2(x-y)^4} + i\theta(x_*)\theta(-y_*)\int d^4z\;\delta(z_*)\frac{(\not{x}-\not{z})}{2\pi^2(x-z)^4}\;\not{p}_2 U_z\frac{(\not{z}-\not{y})}{2\pi^2(y-z)^4}\\ &-\; i\theta(-x_*)\theta(y_*)\int d^4z\;\delta(z_*)\frac{(\not{x}-\not{z})}{2\pi^2(x-z)^4}\;\not{p}_2 U_z^\dagger\frac{(\not{z}-\not{y})}{2\pi^2(x-z)^4}\end{aligned} \tag{97}$$

where $\bar{\psi} = -i\psi^\dagger\gamma_0$. We use Dirac matrices $\gamma^\mu = -i\begin{pmatrix} 0 & \sigma^\mu \\ -\bar{\sigma}_\mu & 0\end{pmatrix}$ where σ^μ are defined in Eq. (18). The LO impact factor is a product of two propagators (97), see Fig. 4 with solid lines representing quarks

$$\begin{aligned}&-(x-y)^4\langle\hat{\bar{\psi}}(x)\gamma_\mu\hat{\psi}(x)\hat{\bar{\psi}}(y)\gamma_\nu\hat{\psi}(y)\rangle \;\overset{x_*>0>y_*}{=}\\ &\frac{1}{16\pi^8}\int d^4z_1 d^4z_2\;\delta(z_{1*})\delta(z_{2*})\frac{(x-y)^4}{X_1^4Y_1^4X_2^4Y_2^4}\;\mathrm{tr}^{\rm spin}\{\gamma_\mu\not{X}_1\not{p}_2\not{Y}_1\gamma_\nu\not{Y}_2\,\not{p}_2\not{X}_2\}\;\mathrm{tr}\{U(z_{1\perp})U^\dagger(z_{2\perp})\}\\ &=\;-\frac{1}{2\pi^6}\int\frac{d^2z_{1\perp}d^2z_{2\perp}}{z_{12}^4}\frac{\mathcal{R}^2}{(\kappa\cdot\zeta_1)(\kappa\cdot\zeta_2)}\frac{\partial^2}{\partial x^\mu\partial y^\nu}\big[-2(\kappa\cdot\zeta_1)(\kappa\cdot\zeta_2)+\kappa^2(\zeta_1\cdot\zeta_2)\big]\mathrm{tr}\{U_{z_{1\perp}}U^\dagger_{z_{2\perp}}\}\end{aligned} \tag{98}$$

Hereafter I use tr{...} to denote the color trace in the fundamental representation (and reserve the notation Tr{...} for the trace in the adjoint representation). The above equation is explicitly Möbius invariant. In addition, it is easy to check that $\frac{\partial}{\partial x_\mu}$(r.h.s)=0.

Feynman diagrams for the photon impact factor are the same as in Fig. 6 but with the solid lines representing quarks. The calculation of the NLO impact factor is similar to the scalar case. The master formula is (cf. Eq. (62))

$$\begin{aligned}&\int d^4z\;\frac{\not{x}-\not{z}}{(x-z)^4}\gamma_\mu\frac{\not{z}-\not{y}}{(z-y)^4}\frac{z_\nu}{z^4} - \mu\leftrightarrow\nu\\ &=\;\frac{\pi^2}{x^2y^2(x-y)^2}\Big[-\not{x}\gamma_\mu\not{y}\Big(\frac{x_\nu}{x^2}+\frac{y_\nu}{y^2}\Big)-\frac{1}{2}(\not{x}\gamma_\mu\gamma_\nu-\gamma_\mu\gamma_\nu\not{y})-2x_\mu y_\nu\frac{\not{x}-\not{y}}{(x-y)^2}\Big]\;-\;\mu\leftrightarrow\nu\end{aligned} \tag{99}$$

which gives the 3-point $\psi\bar{\psi}F_{\mu\nu}$ Green function in the leading order in g. Using this formula one easily obtains

$$\begin{aligned}&-\langle\bar{\psi}(x)\gamma_\mu\psi(x)\bar{\psi}(y)\gamma_\nu\psi(y)\rangle\;\overset{x_*>0>y_*}{=}\;\frac{s}{64\pi^8x_*^2y_*^2}\alpha_s\int d^2z_1\frac{d^2z_2d^2z_3}{z_{13}^2z_{23}^2}[\mathrm{tr}\{U_{z_1}U^\dagger_{z_3}\}\mathrm{tr}\{U_{z_3}U^\dagger_{z_2}\}-N_c\mathrm{tr}\{U_{z_1}U^\dagger_{z_2}\}]\\ &\times\int dz_{1\bullet}dz_{2\bullet}dz_{3\bullet}dz'_{3\bullet}\theta(z_3-z'_3)_\bullet\;\Big[\frac{x_*}{(x-z_1)^2}\frac{(\not{x}-\not{z}_3)}{(x-z_3)^4}\gamma_i\,\not{z}_{13}-2\frac{(\not{x}-\not{z}_1)x_*}{(x-z_1)^4(x-z_3)^2}z_i^{13}\Big]\not{p}_2\frac{\not{z}_1-\not{y}}{(z_1-y)^4}\\ &\times\gamma_\nu\Big[\frac{y_*}{(y-z_2)^2}\frac{(\not{y}-\not{z}_3)}{(y-z'_3)^4}\gamma^i\,\not{z}_{23}-2\frac{(\not{y}-\not{z}_2)y_*}{(y-z_2)^4(y-z'_3)^2}z_{23}^i\Big]\not{p}_2\frac{\not{z}_2-\not{x}}{(z_2-x)^4}\gamma_\mu\end{aligned} \tag{100}$$

Performing integrals over $z_\bullet$'s and taking traces one gets after some algebra the NLO contribution in the form (recall that $z_{ij}^2=-2(\zeta_i\cdot\zeta_j)$ and $\mathcal{Z}_i=-\frac{4}{\sqrt{s}}(\kappa\cdot\zeta_i)$)

$$
\begin{aligned}
&-\hat{\bar{\psi}}(x)\gamma_\mu\hat{\psi}(x)\hat{\bar{\psi}}(y)\gamma_\nu\hat{\psi}(y)\\
&\stackrel{x_*>0>y_*}{=}\quad -\frac{1}{\pi^6}\int\frac{d^2z_1d^2z_2}{z_{12}^4}\;\frac{\mathcal{R}^2}{(\kappa\cdot\zeta_1)(\kappa\cdot\zeta_2)}\Bigg[[\mathrm{tr}\{\hat{U}^Y_{z_1}\hat{U}^{\dagger Y}_{z_2}\}]\frac{\partial^2}{\partial x^\mu\partial y^\nu}\big[-(\kappa\cdot\zeta_1)(\kappa\cdot\zeta_2)+\frac{1}{2}\kappa^2(\zeta_1\cdot\zeta_2)\big]\\
&+\frac{\alpha_s}{16\pi^2}\int d^2z_3[\mathrm{tr}\{\hat{U}^Y_{z_1}\hat{U}^{\dagger Y}_{z_3}\}\mathrm{tr}\{\hat{U}^Y_{z_3}\hat{U}^{\dagger Y}_{z_2}\}-N_c\mathrm{tr}\{\hat{U}^Y_{z_1}\hat{U}^{\dagger Y}_{z_2}\}]\\
&\times\Big\{\frac{(\zeta_1\cdot\zeta_2)}{(\zeta_1\cdot\zeta_3)(\zeta_1\cdot\zeta_3)}\big[\ln\sigma^2 s(\kappa\cdot\zeta_3)^2-i\pi+2C\big]\frac{\partial^2}{\partial x^\mu\partial y^\nu}\big[-2(\kappa\cdot\zeta_1)(\kappa\cdot\zeta_2)+\kappa^2(\zeta_1\cdot\zeta_2)\big]\\
&+\frac{(\kappa\cdot\zeta_2)}{(\kappa\cdot\zeta_3)}\frac{\partial^2}{\partial x^\mu\partial y^\nu}\Big[-\frac{(\kappa\cdot\zeta_1)^2}{(\zeta_1\cdot\zeta_3)}+\frac{(\kappa\cdot\zeta_1)(\kappa\cdot\zeta_3)(\zeta_1\cdot\zeta_2)}{(\zeta_1\cdot\zeta_3)(\zeta_2\cdot\zeta_3)}+\frac{(\kappa\cdot\zeta_1)(\kappa\cdot\zeta_2)}{(\zeta_2\cdot\zeta_3)}-\frac{\kappa^2(\zeta_1\cdot\zeta_2)}{(\zeta_2\cdot\zeta_3)}\Big]\\
&+\frac{(\kappa\cdot\zeta_1)}{(\kappa\cdot\zeta_3)}\frac{\partial^2}{\partial x^\mu\partial y^\nu}\Big[-\frac{(\kappa\cdot\zeta_2)^2}{(\zeta_2\cdot\zeta_3)}+\frac{(\kappa\cdot\zeta_2)(\kappa\cdot\zeta_3)(\zeta_1\cdot\zeta_2)}{(\zeta_1\cdot\zeta_3)(\zeta_2\cdot\zeta_3)}+\frac{(\kappa\cdot\zeta_1)(\kappa\cdot\zeta_2)}{(\zeta_1\cdot\zeta_3)}-\frac{\kappa^2(\zeta_1\cdot\zeta_2)}{(\zeta_1\cdot\zeta_3)}\Big]\\
&+\frac{(\kappa\cdot\zeta_1)^2}{(\kappa\cdot\zeta_3)^2}\frac{\partial^2}{\partial x^\mu\partial y^\nu}\Big[\frac{(\kappa\cdot\zeta_2)(\kappa\cdot\zeta_3)}{(\zeta_1\cdot\zeta_3)}-\frac{\kappa^2(\zeta_2\cdot\zeta_3)}{2(\zeta_1\cdot\zeta_3)}\Big]+\frac{(\kappa\cdot\zeta_2)^2}{(\kappa\cdot\zeta_3)^2}\frac{\partial^2}{\partial x^\mu\partial y^\nu}\Big[\frac{(\kappa\cdot\zeta_1)(\kappa\cdot\zeta_3)}{(\zeta_2\cdot\zeta_3)}-\frac{\kappa^2(\zeta_1\cdot\zeta_3)}{2(\zeta_2\cdot\zeta_3)}\Big]\Big\}\Bigg]
\end{aligned}
\tag{101}
$$

where we have promoted the equation to the operator form. It can be demonstrated that $\frac{\partial}{\partial x^\mu}$[r.h.s. of Eq. (101)] = 0 which reflects the electromagnetic gauge invariance.

As for the N=4 case, it is convenient to re-expand $T\{j_\mu(x)j_\nu(y)\}$ in composite operators obtained by replacement $T^a\to t^a=\frac{\lambda^a}{2}$ (and Tr $\to$ tr) in Eq. (82)

$$
\big[\mathrm{tr}\{\hat{U}_{z_1}\hat{U}^\dagger_{z_2}\}\big]_a\;=\;\mathrm{tr}\{\hat{U}^\sigma_{z_1}\hat{U}^{\dagger\sigma}_{z_2}\}+\frac{\alpha_s}{4\pi^2}\int d^2z_3\;\frac{z_{12}^2}{z_{13}^2z_{23}^2}[\mathrm{tr}\{\hat{U}^\sigma_{z_1}\hat{U}^{\dagger\sigma}_{z_3}\}\mathrm{tr}\{\hat{U}^\sigma_{z_3}\hat{U}^{\dagger\sigma}_{z_2}\}-N_c\mathrm{tr}\{\hat{U}^\sigma_{z_1}\hat{U}^{\dagger\sigma}_{z_2}\}]\ln\frac{4az_{12}^2}{s\sigma^2z_{13}^2z_{23}^2}\;+\;... \tag{102}
$$

where dots stand for α_s^2 terms not displayed here for brevity. In QCD, this composite operator is no longer conformal but still more convenient than the original dipole since the evolution equation for this operator splits into the sum of the conformal part and the running-coupling part proportional to $b=\frac{11}{3}N_c-\frac{2}{3}n_f$ (see the next Section). The final expansion of $T\{j_\mu(x)j_\nu(y)\}$ in composite dipoles (102) has the form (cf. Eq. (71))

$$
\begin{aligned}
&-\hat{\bar{\psi}}(x)\gamma_\mu\hat{\psi}(x)\hat{\bar{\psi}}(y)\gamma_\nu\hat{\psi}(y)\\
&\stackrel{x_*>0>y_*}{=}\quad -\frac{1}{\pi^6}\int\frac{d^2z_1d^2z_2}{z_{12}^4}\;\frac{\mathcal{R}^2}{(\kappa\cdot\zeta_1)(\kappa\cdot\zeta_2)}\Bigg[[\mathrm{tr}\{\hat{U}_{z_1}\hat{U}^\dagger_{z_2}\}]_{a_0}\frac{\partial^2}{\partial x^\mu\partial y^\nu}\big[-(\kappa\cdot\zeta_1)(\kappa\cdot\zeta_2)+\frac{1}{2}\kappa^2(\zeta_1\cdot\zeta_2)\big]\\
&+\frac{\alpha_s}{16\pi^2}\int d^2z_3[\mathrm{tr}\{\hat{U}_{z_1}\hat{U}^\dagger_{z_3}\}\mathrm{tr}\{\hat{U}_{z_3}\hat{U}^\dagger_{z_2}\}-N_c\mathrm{tr}\{\hat{U}_{z_1}\hat{U}^\dagger_{z_2}\}]_{a_0}\\
&\times\Big\{\frac{(\zeta_1\cdot\zeta_2)}{(\zeta_1\cdot\zeta_3)(\zeta_1\cdot\zeta_3)}\Big[\ln\frac{-x_*y_*z_{12}^2\mathcal{Z}_3^2}{(x-y)^2z_{13}^2z_{23}^2}+2C\Big]\frac{\partial^2}{\partial x^\mu\partial y^\nu}\big[-2(\kappa\cdot\zeta_1)(\kappa\cdot\zeta_2)+\kappa^2(\zeta_1\cdot\zeta_2)\big]\\
&+\frac{(\kappa\cdot\zeta_2)}{(\kappa\cdot\zeta_3)}\frac{\partial^2}{\partial x^\mu\partial y^\nu}\Big[-\frac{(\kappa\cdot\zeta_1)^2}{(\zeta_1\cdot\zeta_3)}+\frac{(\kappa\cdot\zeta_1)(\kappa\cdot\zeta_3)(\zeta_1\cdot\zeta_2)}{(\zeta_1\cdot\zeta_3)(\zeta_2\cdot\zeta_3)}+\frac{(\kappa\cdot\zeta_1)(\kappa\cdot\zeta_2)}{(\zeta_2\cdot\zeta_3)}-\frac{\kappa^2(\zeta_1\cdot\zeta_2)}{(\zeta_2\cdot\zeta_3)}\Big]\\
&+\frac{(\kappa\cdot\zeta_1)}{(\kappa\cdot\zeta_3)}\frac{\partial^2}{\partial x^\mu\partial y^\nu}\Big[-\frac{(\kappa\cdot\zeta_2)^2}{(\zeta_2\cdot\zeta_3)}+\frac{(\kappa\cdot\zeta_2)(\kappa\cdot\zeta_3)(\zeta_1\cdot\zeta_2)}{(\zeta_1\cdot\zeta_3)(\zeta_2\cdot\zeta_3)}+\frac{(\kappa\cdot\zeta_1)(\kappa\cdot\zeta_2)}{(\zeta_1\cdot\zeta_3)}-\frac{\kappa^2(\zeta_1\cdot\zeta_2)}{(\zeta_1\cdot\zeta_3)}\Big]\\
&+\frac{(\kappa\cdot\zeta_1)^2}{(\kappa\cdot\zeta_3)^2}\frac{\partial^2}{\partial x^\mu\partial y^\nu}\Big[\frac{(\kappa\cdot\zeta_2)(\kappa\cdot\zeta_3)}{(\zeta_1\cdot\zeta_3)}-\frac{\kappa^2(\zeta_2\cdot\zeta_3)}{2(\zeta_1\cdot\zeta_3)}\Big]+\frac{(\kappa\cdot\zeta_2)^2}{(\kappa\cdot\zeta_3)^2}\frac{\partial^2}{\partial x^\mu\partial y^\nu}\Big[\frac{(\kappa\cdot\zeta_1)(\kappa\cdot\zeta_3)}{(\zeta_2\cdot\zeta_3)}-\frac{\kappa^2(\zeta_1\cdot\zeta_3)}{2(\zeta_2\cdot\zeta_3)}\Big]\Big\}\Bigg]
\end{aligned}
\tag{103}
$$

where we set $a_0=\kappa^{-2}+i\epsilon=\frac{4x_*y_*}{s(x-y)^2}+i\epsilon$ same as for the $\mathcal{N}=4$ case. The explicit expression for four-Wilson-line composite operator $[\mathrm{tr}\{\hat{U}_{z_1}\hat{U}^\dagger_{z_3}\}\mathrm{tr}\{\hat{U}_{z_3}\hat{U}^\dagger_{z_2}\}]_a$ can be obtained from Eq. (84) by usual substitution $T^a\to t^a$ and Tr $\to$ tr. (It is worth noting that at large N_c $[\mathrm{tr}\{\hat{U}_{z_1}\hat{U}^\dagger_{z_3}\}\mathrm{tr}\{\hat{U}_{z_3}\hat{U}^\dagger_{z_2}\}]_a=[\mathrm{tr}\{\hat{U}_{z_1}\hat{U}^\dagger_{z_3}\}]_a[\mathrm{tr}\{\hat{U}_{z_3}\hat{U}^\dagger_{z_2}\}]_a$.) It is easy to see now that the NLO impact factor (103) is Möbius invariant.

B. Evolution of color dipoles in QCD

Second step is the evolution equation for composite operator (102). The types of Feynman diagrams (in the shock-wave background) in QCD are the same as in $\mathcal{N}=4$ SYM (see Fig. 7) but now the solid lines in Figs. 7 VII and VIII denote quarks rather than scalar or gluinos. The result of the evolution of the color dipole with rapidity cutoff (30) is [19]:

$$\begin{aligned}
&\frac{d}{dY}\mathrm{tr}\{\hat U_{z_1}\hat U^\dagger_{z_2}\} \qquad\qquad (104)\\
&= \frac{\alpha_s}{2\pi^2}\int d^2z\ \frac{z_{12}^2}{z_{13}^2z_{23}^2}\Big\{1+\frac{\alpha_s}{4\pi}\Big[b\ln z_{12}^2\mu^2 - b\frac{z_{13}^2-z_{23}^2}{z_{12}^2}\ln\frac{z_{13}^2}{z_{23}^2}+(\frac{67}{9}-\frac{\pi^2}{3})N_c-\frac{10}{9}n_f\\
&\qquad -2N_c\ln\frac{z_{13}^2}{z_{12}^2}\ln\frac{z_{23}^2}{z_{12}^2}\Big]\Big\}\ [\mathrm{tr}\{\hat U_{z_1}\hat U^\dagger_{z_3}\}\mathrm{tr}\{\hat U_{z_3}\hat U^\dagger_{z_2}\}-N_c\mathrm{tr}\{\hat U_{z_1}\hat U^\dagger_{z_2}\}]\\
&+\frac{\alpha_s^2}{16\pi^4}\int d^2z_3d^2z_4\Big[\Big(-\frac{4}{z_{34}^4}+\Big\{2\frac{z_{13}^2z_{24}^2+z_{14}^2z_{23}^2-4z_{12}^2z_{34}^2}{z_{34}^4[z_{13}^2z_{24}^2-z_{14}^2z_{23}^2]}+\frac{z_{12}^4}{z_{13}^2z_{24}^2-z_{14}^2z_{23}^2}\Big[\frac{1}{z_{13}^2z_{24}^2}+\frac{1}{z_{23}^2z_{14}^2}\Big]\\
&+\frac{z_{12}^2}{z_{34}^2}\Big[\frac{1}{z_{13}^2z_{24}^2}-\frac{1}{z_{14}^2z_{23}^2}\Big]\Big\}\ln\frac{z_{13}^2z_{24}^2}{z_{14}^2z_{23}^2}\Big)[\mathrm{tr}\{\hat U_{z_1}\hat U^\dagger_{z_3}\}\mathrm{tr}\{\hat U_{z_3}\hat U^\dagger_{z_4}\}\mathrm{tr}\{\hat U_{z_4}\hat U^\dagger_{z_2}\}-\mathrm{tr}\{\hat U_{z_1}\hat U^\dagger_{z_3}\hat U_{z_4}U^\dagger_{z_2}\hat U_{z_3}\hat U^\dagger_{z_4}\}-(z_4\to z_3)]\\
&+\Big\{\frac{z_{12}^2}{z_{34}^2}\Big[\frac{1}{z_{13}^2z_{24}^2}+\frac{1}{z_{23}^2z_{14}^2}\Big]-\frac{z_{12}^4}{z_{13}^2z_{24}^2z_{14}^2z_{23}^2}\Big\}\ln\frac{z_{13}^2z_{24}^2}{z_{14}^2z_{23}^2}\ \mathrm{tr}\{\hat U_{z_1}\hat U^\dagger_{z_3}\}\mathrm{tr}\{\hat U_{z_3}\hat U^\dagger_{z_4}\}\mathrm{tr}\{\hat U_{z_4}\hat U^\dagger_{z_2}\}\\
&+4n_f\Big\{\frac{4}{z_{34}^4}-2\frac{z_{14}^2z_{23}^2+z_{24}^2z_{13}^2-z_{12}^2z_{34}^2}{z_{34}^4(z_{13}^2z_{24}^2-z_{14}^2z_{23}^2)}\ln\frac{z_{13}^2z_{24}^2}{z_{14}^2z_{23}^2}\Big\}\mathrm{tr}\{t^a\hat U_{z_1}t^b\hat U^\dagger_{z_2}\}[\mathrm{tr}\{t^a\hat U_{z_3}t^b\hat U^\dagger_{z_4}\}-(z_4\to z_3)]\Big]
\end{aligned}$$

where we use the $\overline{MS}$ scheme. The NLO kernel is a sum of the running-coupling part (proportional to b), the non-conformal double-log term $\sim\ln\frac{z_{12}^2}{z_{13}^2}\ln\frac{z_{12}^2}{z_{13}^2}$ (same as in $\mathcal{N}=4$ case) and the three conformal terms which depend on the two four-point conformal ratios $\frac{z_{13}^2z_{24}^2}{z_{14}^2z_{23}^2}$ and $\frac{z_{12}^2z_{34}^2}{z_{13}^2z_{24}^2}$.

A natural guess for QCD result as opposed to $\mathcal{N}=4$ answer would be some sort of tree-level conformal structure which "get dressed" by the running coupling constant. At the NLO level, this would correspond to the sum of the conformal part and the running-coupling part proportional to b. As we see, the Eq. (104) does not quite look like such sum due to the presence of the double-log term. It turns out, however, that if one rewrites the evolution equation (104) in terms of composite operators (102), the NLO kernel separates into the sum of conformal and running-coupling parts [14]:

$$\begin{aligned}
2a\frac{d}{da}\big[\mathrm{tr}\{\hat U_{z_1}\hat U^\dagger_{z_2}\}\big]_a &= \frac{\alpha_s}{2\pi^2}\int d^2z_3\ \frac{z_{12}^2}{z_{13}^2z_{23}^2}\big[\mathrm{tr}\{\hat U_{z_1}\hat U^\dagger_{z_3}\}\mathrm{tr}\{\hat U_{z_3}\hat U^\dagger_{z_2}\}-N_c\mathrm{tr}\{\hat U_{z_1}\hat U^\dagger_{z_2}\}\big]_a\\
&\times\Big\{1+\frac{\alpha_s}{4\pi}\Big[b(\ln\frac{z_{12}^2\mu^2}{4}+2C)-b\frac{z_{13}^2-z_{23}^2}{z_{12}^2}\ln\frac{z_{13}^2}{z_{23}^2}+(\frac{67}{9}-\frac{\pi^2}{3})N_c-\frac{10}{9}n_f\Big]\Big\}\\
&+\frac{\alpha_s^2}{16\pi^4}\int\frac{d^2z_3d^2z_4}{z_{34}^4}\Big[\Big\{\Big(-2+2\frac{z_{12}^2z_{34}^2}{z_{13}^2z_{24}^2}\ln\frac{z_{12}^2z_{34}^2}{z_{14}^2z_{23}^2}+\Big[\frac{z_{12}^2z_{34}^2}{z_{13}^2z_{24}^2}\big(1+\frac{z_{12}^2z_{34}^2}{z_{13}^2z_{24}^2-z_{14}^2z_{23}^2}\big)+\frac{2z_{13}^2z_{24}^2-4z_{12}^2z_{34}^2}{z_{13}^2z_{24}^2-z_{14}^2z_{23}^2}\Big]\ln\frac{z_{13}^2z_{24}^2}{z_{14}^2z_{23}^2}\Big)\\
&+\big(z_3\leftrightarrow z_4\big)\Big\}\ \big[\big(\mathrm{tr}\{\hat U_{z_1}\hat U^\dagger_{z_3}\}\mathrm{tr}\{\hat U_{z_3}\hat U^\dagger_{z_4}\}\mathrm{tr}\{\hat U_{z_4}\hat U^\dagger_{z_2}\}-\mathrm{tr}\{\hat U_{z_1}\hat U^\dagger_{z_3}\hat U_{z_4}\hat U^\dagger_{z_2}\hat U_{z_3}\hat U^\dagger_{z_4}\}\big)-(z_4\to z_3)\big]_a\\
&+\frac{z_{12}^2z_{34}^2}{z_{13}^2z_{24}^2}\Big\{2\ln\frac{z_{12}^2z_{34}^2}{z_{14}^2z_{23}^2}+\Big[1+\frac{z_{12}^2z_{34}^2}{z_{13}^2z_{24}^2-z_{14}^2z_{23}^2}\Big]\ln\frac{z_{13}^2z_{24}^2}{z_{14}^2z_{23}^2}\Big\}\big[\mathrm{tr}\{\hat U_{z_1}\hat U^\dagger_{z_3}\}\mathrm{tr}\{\hat U_{z_3}\hat U^\dagger_{z_4}\}\mathrm{tr}\{\hat U_{z_4}\hat U^\dagger_{z_2}\}-z_3\leftrightarrow z_4\big]_a\Big]\\
&+\frac{\alpha_s^2n_f}{2\pi^4}\int\frac{d^2z_3d^2z_4}{z_{34}^4}\Big\{2-\frac{z_{13}^2z_{24}^2+z_{23}^2z_{14}^2-z_{12}^2z_{34}^2}{z_{13}^2z_{24}^2-z_{14}^2z_{23}^2}\ln\frac{z_{13}^2z_{24}^2}{z_{14}^2z_{23}^2}\Big\}[\mathrm{tr}\{t^a\hat U_{z_1}t^b\hat U^\dagger_{z_2}\}\mathrm{tr}\{t^a\hat U_{z_3}t^b(\hat U^\dagger_{z_4}-\hat U_{z_3})\}]_a.
\end{aligned}\qquad (105)$$

Following the analysis of Ref. [19] I will outline how the above kernel reproduces the NLO BFKL eigenvalues [3] (for details see the Appendix).

In the two-gluon approximation we get

$$\mathrm{tr}\{\hat U^Y_{z_1}\hat U^{\dagger Y}_{z_3}\}\mathrm{tr}\{\hat U^Y_{z_3}\hat U^{\dagger Y}_{z_2}\}-N_c\mathrm{tr}\{\hat U^Y_{z_1}\hat U^{\dagger Y}_{z_2}\} = -N_c\big[\hat{\mathcal{U}}^Y(z_1,z_3)+\hat{\mathcal{U}}^Y(z_2,z_3)-\hat{\mathcal{U}}^Y(z_1,z_2)\big] \qquad (106)$$

where

$$\hat{\mathcal{U}}^Y(x_\perp,y_\perp) = 1-\frac{1}{N_c}\mathrm{tr}\{\hat{U}^Y(x_\perp)\hat{U}^{\dagger Y}(y_\perp)\} \tag{107}$$

is the color dipole in the fundamental representation. In this approximation the composite dipole (102) reduces to (cf. Eq. (69))

$$\begin{aligned}
\hat{\mathcal{U}}_a(z_1,z_2) \;=\; & \mathcal{U}^Y(z_1,z_2)+\frac{\alpha_sN_c}{4\pi^2}\int d^2z_3\,\frac{z_{12}^2}{z_{13}^2z_{23}^2}[\hat{\mathcal{U}}^Y(z_1,z_3)+\hat{\mathcal{U}}^Y(z_2,z_3)-\hat{\mathcal{U}}^Y(z_1,z_2)]\ln\Big(\frac{4az_{12}^2}{\sigma^2sz_{13}^2z_{23}^2}\Big)+\frac{\alpha_s^2N_c^2}{16\pi^4}\\
&\times\int d^2z_3\,\frac{z_{12}^2}{z_{13}^2z_{23}^2}\Big[\frac{b}{N_c}\Big(\ln z_{12}^2\mu^2-\frac{z_{13}^2-z_{23}^2}{z_{12}^2}\ln\frac{z_{13}^2}{z_{23}^2}\Big)+\frac{67}{9}-\frac{\pi^2}{3}-\frac{10n_f}{9N_c}\Big][\hat{\mathcal{U}}^Y(z_1,z_3)+\hat{\mathcal{U}}^Y(z_2,z_3)-\hat{\mathcal{U}}^Y(z_1,z_2)]\ln\frac{4a}{\sigma^2s}\\
&+\frac{\alpha_s^2N_c^2}{16\pi^4}\int\frac{d^2z_3d^2z_4}{z_{34}^4}\Big\{-2+\frac{z_{13}^2z_{24}^2+z_{14}^2z_{23}^2-4z_{12}^2z_{34}^2}{z_{13}^2z_{24}^2-z_{14}^2z_{23}^2}\ln\frac{z_{13}^2z_{24}^2}{z_{14}^2z_{23}^2}-\frac{n_f}{N_c^3}\Big[2-\frac{z_{14}^2z_{23}^2+z_{24}^2z_{13}^2-z_{12}^2z_{34}^2}{z_{14}^2z_{23}^2-z_{24}^2z_{13}^2}\ln\frac{z_{14}^2z_{23}^2}{z_{24}^2z_{13}^2}\Big]\\
&+\frac{z_{12}^2z_{34}^2}{z_{13}^2z_{24}^2}\Big[2\ln\frac{z_{12}^2z_{34}^2}{z_{14}^2z_{23}^2}+\Big(1+\frac{z_{12}^2z_{34}^2}{z_{13}^2z_{24}^2-z_{14}^2z_{23}^2}\Big)\ln\frac{z_{13}^2z_{24}^2}{z_{14}^2z_{23}^2}\Big]\Big\}\,\hat{\mathcal{U}}^Y(z_3,z_4)\ln\frac{4a}{\sigma^2s}+\frac{\alpha_s^2N_c^2}{4\pi^2}\zeta(3)\,\hat{\mathcal{U}}^Y(z_1,z_2)\ln\frac{4a}{\sigma^2s}\\
&+\frac{\alpha_s^2N_c^2}{32\pi^4}\int d^2z_3d^2z_4\,\frac{z_{12}^2}{z_{13}^2z_{23}^2}\Big\{\frac{z_{13}^2}{z_{14}^2z_{34}^2}[\hat{\mathcal{U}}^Y(z_1,z_4)+\hat{\mathcal{U}}^Y(z_3,z_4)-\hat{\mathcal{U}}^Y(z_1,z_3)]\ln^2\Big(\frac{4az_{13}^2}{\sigma^2sz_{14}^2z_{34}^2}\Big)+\frac{z_{23}^2}{z_{34}^2z_{24}^2}[\hat{\mathcal{U}}^Y(z_3,z_4)\\
&+\hat{\mathcal{U}}^Y(z_2,z_4)-\hat{\mathcal{U}}^Y(z_2,z_3)]\ln^2\Big(\frac{4az_{23}^2}{\sigma^2sz_{24}^2z_{34}^2}\Big)-\frac{z_{12}^2}{z_{14}^2z_{24}^2}[\hat{\mathcal{U}}^Y(z_1,z_4)+\hat{\mathcal{U}}^Y(z_2,z_4)-\hat{\mathcal{U}}^Y(z_1,z_2)]\ln^2\Big(\frac{4az_{12}^2}{\sigma^2sz_{14}^2z_{24}^2}\Big)\Big\}
\end{aligned}\tag{108}$$

It is easy to see that $\frac{d}{dY}$ ($\equiv\sigma\frac{d}{d\sigma}$) of the r.h.s. vanishes.

The evolution equation (105) turns into

$$\begin{aligned}
2a\frac{d}{da}\hat{\mathcal{U}}_a(z_1,z_2) \;=\; & \frac{\alpha_sN_c}{2\pi^2}\int d^2z_3\,\frac{z_{12}^2}{z_{13}^2z_{23}^2}\Big[1\\
&+\frac{\alpha_s}{4\pi}\Big[b\Big(\frac{\ln z_{12}^2\mu^2}{4}+2C\Big)-b\frac{z_{13}^2-z_{23}^2}{z_{12}^2}\ln\frac{z_{13}^2}{z_{23}^2}+\Big(\frac{67}{9}-\frac{\pi^2}{3}\Big)N_c-\frac{10}{9}n_f\Big]\Big[\hat{\mathcal{U}}_a(z_1,z_3)+\hat{\mathcal{U}}_a(z_2,z_3)-\hat{\mathcal{U}}_a(z_1,z_2)\Big]\\
&+\frac{\alpha_s^2N_c^2}{8\pi^4}\int\frac{d^2z_3d^2z_4}{z_{34}^2}\Big\{2\frac{z_{12}^2z_{34}^2}{z_{13}^2z_{24}^2}\ln\frac{z_{12}^2z_{34}^2}{z_{14}^2z_{23}^2}+\frac{z_{12}^2z_{34}^2}{z_{13}^2z_{24}^2}\Big(1+\frac{z_{12}^2z_{34}^2}{z_{13}^2z_{24}^2-z_{14}^2z_{23}^2}\Big)\ln\frac{z_{13}^2z_{24}^2}{z_{14}^2z_{23}^2}-\frac{3z_{12}^2z_{34}^2}{z_{13}^2z_{24}^2-z_{14}^2z_{23}^2}\ln\frac{z_{13}^2z_{24}^2}{z_{14}^2z_{23}^2}\\
&+\Big(1+\frac{n_f}{N_c^3}\Big)\Big(\frac{z_{13}^2z_{24}^2+z_{14}^2z_{23}^2-z_{12}^2z_{34}^2}{z_{13}^2z_{24}^2-z_{14}^2z_{23}^2}\ln\frac{z_{13}^2z_{24}^2}{z_{14}^2z_{23}^2}-2\Big)\Big\}\hat{\mathcal{U}}_a(z_3,z_4)+\frac{3\alpha_s^2N_c^2}{2\pi^2}\zeta(3)\hat{\mathcal{U}}_a(z_1,z_2)
\end{aligned}\tag{109}$$

where we used formula [14]

$$\int d^2z_4\,\Big\{\frac{z_{12}^2}{z_{13}^2z_{24}^2z_{34}^2}\Big(2\ln\frac{z_{12}^2z_{34}^2}{z_{14}^2z_{23}^2}+\Big[1+\frac{z_{12}^2z_{34}^2}{z_{13}^2z_{24}^2-z_{14}^2z_{23}^2}\Big]\ln\frac{z_{13}^2z_{24}^2}{z_{14}^2z_{23}^2}\Big)-z_3\leftrightarrow z_4\Big\}\;=\;12\pi\zeta(3)[\delta(z_{23})-\delta(z_{13})] \tag{110}$$

For the case of forward scattering $\langle\hat{\mathcal{U}}(x,y)\rangle=\mathcal{U}(x-y)$ and the linearized equation (109) can be reduced to an integral equation with respect to one variable $z\equiv z_{12}$. Using integrals (104)-(106) from Ref. [19] and the integral

$$\int d\tilde{z}\frac{1}{\tilde{z}^2(z-z'-\tilde{z})^2}\ln\frac{z^2z'^2}{(z-\tilde{z}^2)(z'-\tilde{z}^2)}\;=\;-\frac{\pi}{(z-z')^2}\ln^2\frac{z^2}{z'^2}$$

we obtain

$$\begin{aligned}
2a\frac{d}{da}\mathcal{U}_a(z) \;=\; & \frac{\alpha_sN_c}{2\pi^2}\int d^2z\,\frac{z^2}{(z-z')^2z'^2}\Big\{1\\
&+\frac{\alpha_s}{4\pi}\Big[b\Big(\ln\frac{z^2\mu^2}{4}+2C\Big)-b\frac{(z-z')^2-z'^2}{z^2}\ln\frac{(z-z')^2}{z'^2}+\Big(\frac{67}{9}-\frac{\pi^2}{3}\Big)N_c-\frac{10}{9}n_f\Big][\mathcal{U}_a(z-z')+\mathcal{U}_a(z')-\mathcal{U}_a(z)]\\
&+\frac{\alpha_s^2N_c^2}{4\pi^3}\int d^2z'\,\frac{z^2}{z'^2}\Big[-\frac{1}{(z-z')^2}\ln^2\frac{z^2}{z'^2}+F(z,z')+\Phi(z,z')\Big]\,\mathcal{U}_a(z')+3\frac{\alpha_s^2N_c^2}{2\pi^2}\zeta(3)\mathcal{U}_a(z)
\end{aligned}\tag{111}$$

where

$$\begin{aligned}
F(z,z') \;=\; & \Big(1+\frac{n_f}{N_c^3}\Big)\frac{3(z,z')^2-2z^2z'^2}{16z^2z'^2}\Big(\frac{2}{z^2}+\frac{2}{z'^2}+\frac{z^2-z'^2}{z^2z'^2}\ln\frac{z^2}{z'^2}\Big)\\
&-\Big[3+\Big(1+\frac{n_f}{N_c^3}\Big)\Big(1-\frac{(z^2+z'^2)^2}{8z^2z'^2}+\frac{3z^4+3z'^4-2z^2z'^2}{16z^4z'^4}(z,z')^2\Big)\Big]\int_0^\infty dt\frac{1}{z^2+t^2z'^2}\ln\frac{1+t}{|1-t|}
\end{aligned}\tag{112}$$

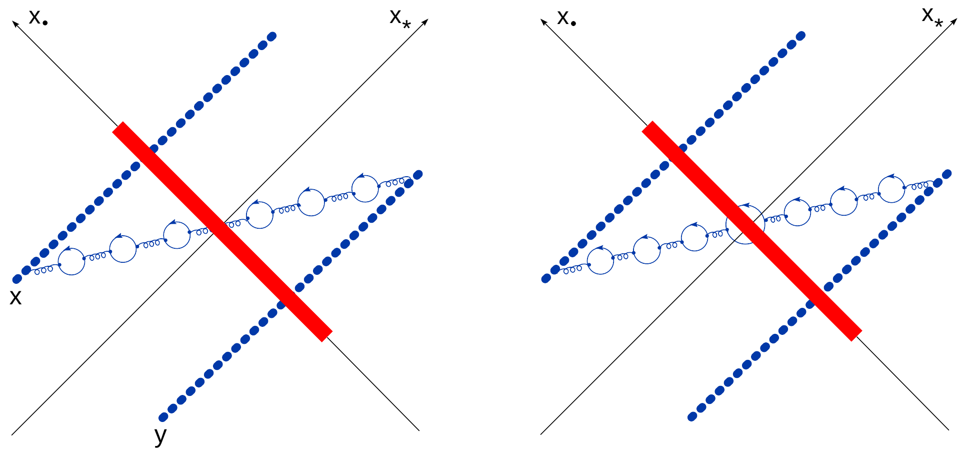

FIG. 9: Renormalon bubble chain of quark loops.

and

$$\Phi(z,z') = \frac{(z^2-z'^2)}{(z-z')^2(z+z')^2}\Big[\ln\frac{z^2}{z'^2}\ln\frac{z^2z'^2(z-z')^4}{(z^2+z'^2)^4}+2\mathrm{Li}_2\Big(-\frac{z'^2}{z^2}\Big)-2\mathrm{Li}_2\Big(-\frac{z^2}{z'^2}\Big)\Big]$$
$$-\Big(1-\frac{(z^2-z'^2)^2}{(z-z')^2(z+z')^2}\Big)\Big[\int_0^1-\int_1^\infty\Big]\frac{du}{(z-z'u)^2}\ln\frac{u^2z'^2}{z^2} \tag{113}$$

The function $-\frac{1}{(q-q')^2}\ln^2\frac{q^2}{q'^2}+F(q,q')+\Phi(q,q')$ enters the NLO BFKL equation in the momentum space [3] and since the eigenfunctions of the forward BFKL equation are powers both in the coordinate and momentum space, it is clear that the corresponding eigenvalues coincide. Moreover, it can be demonstrated explicitly that

$$\frac{1}{4\pi^2}\int d^2qd^2q'\ e^{i(q,z)-i(q',z')}\Big[-\frac{1}{(q-q')^2}\ln^2\frac{q^2}{q'^2}+F(q,q')+\Phi(q,q')\Big] = -\frac{1}{(z-z')^2}\ln^2\frac{z^2}{z'^2}+F(z,z')+\Phi(z,z') \tag{114}$$

so the conformal ($\mathcal{N}=4$) part of the forward kernel looks the same in the coordinate and in the momentum representation. As to the running-coupling part (the first term in the r.h.s. of Eq. (120)), in the Appendix we demonstrate that it also agrees with the eigenvalues (3).

C. Argument of the coupling constant in the BK equation

I will not discuss here the steps 3 and 4 of our OPE program. The reason is that in DIS from nucleon or nucleus the evolution of color dipoles is non-linear and the analytic solution is not known at the present time. Even in the simpler case of forward $\gamma^*\gamma^*$ or onium-onium scattering where the dipole evolution is described by linear NLO BFKL equation, it is impossible to solve this equation since we do not know the argument of the coupling constant. Moreover, it is not known how to solve analytically this equation even if we take some simple model for the argument of coupling constant like the size of the parent dipole.

Still, the first step towards the solution would be to figure out the argument of coupling constant in the NLO BFKL equation. To get an argument of coupling constant we can use the renormalon-based approach (for a review, see Ref. [37]) and trace the quark part of the β-function proportional to n_f. In the leading log approximation $\alpha_s\ln\frac{p^2}{\mu^2}\sim 1,\ \alpha_s\ll 1$ the quark part of the β-function comes from the bubble chain of quark loops in the shock-wave background. We can either have no intersection of quark loop with the shock wave (see Fig. 9a) or we may have one of the loops in the shock-wave background (see Fig. 9b).

The sum of these diagrams yields

$$\frac{d}{dY}\langle\mathrm{Tr}\{\hat U_{z_1}\hat U^\dagger_{z_2}\}\rangle = -2\alpha_s\mathrm{Tr}\{t^aU_{z_1}t^bU^\dagger_{z_2}\}\int d\!\!{}^-{}^2p\,d\!\!{}^-{}^2l\ [e^{i(p,z_1)_\perp}-e^{i(p,z_2)_\perp}][e^{-i(p-l,z_1)_\perp}-e^{-i(p-l,z_2)_\perp}]$$
$$\times\ \frac{1}{p^2(1+\frac{\alpha_s}{6\pi}\ln\frac{\mu^2}{p^2})}\Big(1-\frac{\alpha_sn_f}{6\pi}\ln\frac{l^2}{\mu^2}\Big)\partial^2_\perp U^{ab}(l)\frac{1}{(p-l)^2(1+\frac{\alpha_s}{6\pi}\ln\frac{\mu^2}{(p-l)^2})} \tag{115}$$

where we have left only the β-function part of the quark loop. Replacing the quark part of the β-function $-\frac{\alpha_s}{6\pi}n_f\ln\frac{p^2}{\mu^2}$ by the total contribution $\frac{\alpha_s}{4\pi}b\ln\frac{p^2}{\mu^2}$ we get

$$\begin{aligned}\frac{d}{dY}\langle\mathrm{Tr}\{\hat U_{z_1}\hat U^\dagger_{z_2}\}\rangle \;&=\; -2\mathrm{Tr}\{t^aU_{z_1}t^bU^\dagger_{z_2}\}\\ \times\int d\!\!\!^-{}^2p\, d\!\!\!^-{}^2q\;[e^{i(p,z_1)_\perp}-e^{i(p,z_2)_\perp}][e^{-i(p-l,z_1)_\perp}-e^{-i(p-l,z_2)_\perp}]&\frac{\alpha_s(p^2)}{p^2}\alpha_s^{-1}(l^2)\partial_\perp^2U^{ab}(q)\frac{\alpha_s((p-l)^2)}{(p-l)^2}\end{aligned}\tag{116}$$

In principle, one should also include the "renormalon dressing" of α_s^2 in Eq. (105). We think, however, that they form a separate contribution which has nothing to do with the argument of the BK equation.

To go to the coordinate space, we expand the coupling constants in Eq. (116) in powers of $\alpha_s=\alpha_s(\mu^2)$, i.e. return back to Eq. (115) with $\frac{\alpha_s}{6\pi}n_f\rightarrow -b\frac{\alpha_s}{4\pi}$. Unfortunately, the Fourier transformation to the coordinate space can be performed explicitly only for a couple of first terms of the expansion $\alpha_s(p^2)\simeq\alpha_s-\frac{b\alpha_s}{4\pi}\ln p^2/\mu^2+(\frac{b\alpha_s}{4\pi}\ln p^2/\mu^2)^2$. With this accuracy [18, 38]

$$\frac{d}{dY}\mathrm{Tr}\{\hat U_{z_1}\hat U^\dagger_{z_2}\} \;=\; \frac{\alpha_s(z_{12}^2)}{2\pi^2}\int d^2z\;[\mathrm{Tr}\{\hat U_{z_1}\hat U^\dagger_{z_3}\}\mathrm{Tr}\{\hat U_{z_3}\hat U^\dagger_{z_2}\}-N_c\mathrm{Tr}\{\hat U_{z_1}\hat U^\dagger_{z_2}\}]\tag{117}$$

$$\times\Big[\frac{z_{12}^2}{z_{13}^2z_{23}^2}+\frac{1}{z_{13}^2}\Big(\frac{\alpha_s(z_{13}^2)}{\alpha_s(z_{23}^2)}-1\Big)+\frac{1}{z_{23}^2}\Big(\frac{\alpha_s(z_{23}^2)}{\alpha_s(z_{13}^2)}-1\Big)\Big]+\dots\tag{118}$$

where dots stand for the remaining α_s^2 terms. (Here we promoted Wilson lines in the r.h.s. to operators).

When the sizes of the dipoles are very different the kernel of the above equation reduces to

$$\begin{array}{ll}\frac{\alpha_s(z_{12}^2)}{2\pi^2}\frac{z_{12}^2}{z_{13}^2z_{23}^2} & |z_{12}|\ll|z_{13}|,|z_{23}|\\ \frac{\alpha_s(z_{13})^2)}{2\pi^2z_{13}^2} & |z_{13}\ll|z_{12}|,|z_{23}|\\ \frac{\alpha_s(z_{23})^2)}{2\pi^2z_{23}^2} & |z_{23}|\ll|z_{12}|,|z_{13}|\end{array}\tag{119}$$

so the argument of the coupling constant is the size of smallest dipole. The numerical approach to solution of the the NLO BK equation with this running coupling constant is presented in Ref. [39].

VI. CONCLUSIONS

The main conclusion is that the rapidity factorization and high-energy operator expansion in color dipoles works at the NLO level. There are many examples of the factorization which are fine at the leading order but fail at the NLO level. I believe that the high-energy OPE has the same status as usual light-cone expansion in light-ray operators so one can calculate the high-energy amplitudes level by level in perturbation theory. As an outlook my collaborator G. Chirilli and I intend to apply the NLO high-energy operator expansion for the description of QCD amplitudes. (The intermediate result for the impact factor (103) is the first step of that program). There are many papers devoted to analysis of the high-energy amplitudes in QCD at the NLO level (see e.g. Refs. [6, 40, 41]) but all of them use traditional calculation of Feynman diagrams in momentum space. In our opinion, the high-energy OPE in color dipoles is technically more simple and gives us an opportunity to use an approximate tree-level conformal invariance in QCD. Moreover, the exact prescription for separating the coefficient functions (impact factors) and matrix elements is somewhat tricky in the traditional approach while it comes naturally in the framework of OPE logic. When finished, the calculation of the photon impact factor for the structure function $F_2(x)$ of deep inelastic scattering will compete the analysis of the small-x behavior of DIS structure functions at the NLO level. The study is in progress.

The author is grateful to L.N. Lipatov for more than thirty years of valuable discussions and guidance. This work was supported by contract DE-AC05-06OR23177 under which the Jefferson Science Associates, LLC operate the Thomas Jefferson National Accelerator Facility.

VII. APPENDIX: COMPARISON TO NLO BFKL IN QCD

We will compare our evolution equation for $\mathcal{U}^Y$ to similar equation obtained from the NLO BFKL momentum-space analysis [3, 4]. The linearized version of the Eq. (104) has the form (cf Eq. (111):

$$\begin{aligned}\frac{d}{dY}\mathcal{U}^Y(z) &= \frac{\alpha_sN_c}{2\pi^2}\int d^2z\ \frac{z^2}{(z-z')^2z'^2}\Big\{1+\ \frac{\alpha_s}{4\pi}\Big[b\big(\ln\frac{z^2\mu^2}{4}+2C\big)\\ &- b\frac{(z-z')^2-z'^2}{z^2}\ln\frac{(z-z')^2}{z'^2}+(\frac{67}{9}-\frac{\pi^2}{3})N_c-\frac{10}{9}n_f-2N_c\ln\frac{z^2}{z'^2}\ln\frac{z^2}{(z-z')^2}\Big][\mathcal{U}^Y(z-z')+\mathcal{U}^Y(z')-\mathcal{U}^Y(z)]\\ &+\frac{\alpha_s^2N_c^2}{4\pi^3}\int d^2z'\ \frac{z^2}{z'^2}[F(z,z')+\Phi(z,z')]\ \mathcal{U}^Y(z')+\frac{\alpha_s^2N_c^2}{2\pi^2}\zeta(3)\mathcal{U}^Y(z)\end{aligned}\tag{120}$$

where $F(z,z')$ and $\Phi(z,z')$ are given by Eqs. (112) and (113), respectively.

To compare the eigenvalues of the Eq. (120) with NLO BFKL we expand $\mathcal{U}^Y(x,0)$ in eigenfunctions (35)

$$\langle\hat{\mathcal{U}}^Y(x_\perp,0)\rangle=\sum_{n=-\infty}^{\infty}\int_{-\frac12-i\infty}^{-\frac12+i\infty}\frac{d\gamma}{2\pi i}\ e^{in\phi}(x_\perp^2\mu^2)^\gamma\ \langle\hat{\mathcal{U}}^Y(n,\gamma)\rangle\ ,\tag{121}$$

compute the evolution of $\langle\hat{\mathcal{U}}(n,\gamma)\rangle$ from Eq. (120) and compare it to the calculation based on the NLO BFKL results from [3, 28]. (Here we will not consider the quark part of the NLO BK kernel - the agreement of that part with the n_f term in the NLO BFKL kernel was proved in Ref. [42]).

The relevant integrals have the form

$$\begin{aligned}\frac{1}{2\pi}\int d^2z\ [2(z^2/x^2)^\gamma e^{in\phi}-1]\frac{x^2}{(x-z)^2z^2}\ &=\ \chi(n,\gamma)\\ \frac{1}{\pi}\int d^2z\ [2(z^2/x^2)^\gamma e^{in\phi}-1]\Big(\frac{1}{(x-z)^2}-\frac{1}{z^2}\Big)\ln\frac{(x-z)^2}{z^2}\ &=\ \chi^2(n,\gamma)-\chi'(n,\gamma)-\frac{4\gamma\chi(\gamma)}{\gamma^2-\frac{n^2}{4}}\\ \frac{1}{\pi}\int d^2z\ (z^2/x^2)^\gamma\frac{x^2}{(x-z)^2z^2}e^{in\phi}\ln\frac{(x-z)^2}{x^2}\ln\frac{z^2}{x^2}\ &=\ \frac12\chi''(n,\gamma)+\chi'(n,\gamma)\chi(n,\gamma)\end{aligned}\tag{122}$$

where $\chi(n,\gamma)=-2C-\psi(\gamma+\frac{n}{2})-\psi(1-\gamma+\frac{n}{2})$, and

$$\begin{aligned}&\frac{1}{\pi}\int d^2z'\ (z'^2/z^2)^{\gamma-1}e^{in\phi'}F(z,z')\\ &=\ \Big\{-\Big[3+\Big(1+\frac{n_f}{N_c^3}\Big)\frac{2+3\gamma\bar\gamma}{(3-2\gamma)(1+2\gamma)}\Big]\delta_{0n}+\Big(1+\frac{n_f}{N_c^3}\Big)\frac{\gamma\bar\gamma}{2(3-2\gamma)(1+2\gamma)}\delta_{2n}\Big\}\frac{\pi^2\cos\pi\gamma}{(1-2\gamma)\sin^2\pi\gamma}\ \equiv\ F(n,\gamma)\end{aligned}$$

$$\frac{1}{2\pi}\int d^2z\ (z'^2/z^2)^{\gamma-1}e^{in\phi'}\Phi(z,z')\ =\ -\Phi(n,\gamma)-\Phi(n,1-\gamma)\tag{123}$$

where [28]

$$\begin{aligned}\Phi(n,\gamma)\ &=\ \int_0^1\frac{dt}{1+t}\ t^{\gamma-1+\frac{n}{2}}\Big\{\frac{\pi^2}{12}-\frac12\psi'\Big(\frac{n+1}{2}\Big)-\mathrm{Li}_2(t)-\mathrm{Li}_2(-t)\\ &-\Big(\psi(n+1)-\psi(1)+\ln(1+t)+\sum_{k=1}^\infty\frac{(-t)^k}{k+n}\Big)\ln t-\sum_{k=1}^\infty\frac{t^k}{(k+n)^2}[1-(-1)^k]\Big\}\end{aligned}\tag{124}$$

(note that $\chi(0,\frac12+i\nu)\equiv\chi(\nu)$ and $\Phi(0,\frac12+i\nu)\equiv\Phi(\nu)$, see Eq. (4)). The convenient way to calculate the integrals over angle ϕ is to represent $\cos n\phi$ as $T_n(\cos\phi)$ and use formulas for the integration of Chebyshev polynomials from Ref. [28].

Using integrals (122) - (123) one easily obtains the evolution equation for $\mathcal{U}(n,\gamma)$ in the form

$$\begin{aligned}&\frac{d}{dY}\langle\hat{\mathcal{U}}^Y(n,\gamma)\rangle\\ &=\frac{\alpha_sN_c}{\pi}\Big\{\Big[1-\frac{b\alpha_s}{4\pi}\big(\frac{d}{d\gamma}+\ln4-2C\big)+\frac{\alpha_sN_c}{4\pi}\Big(\frac{67}{9}-\frac{\pi^2}{3}-\frac{10}{9}\frac{n_f}{N_c^3}\Big)\Big]\chi(n,\gamma)+\frac{\alpha_sb}{4\pi}\Big[\frac12\chi^2(n,\gamma)-\frac12\chi'(n,\gamma)-\frac{2\gamma\chi(n,\gamma)}{\gamma^2-\frac{n^2}{4}}\Big]\\ &+\frac{\alpha_sN_c}{4\pi}\Big[-\chi''(n,\gamma)-2\chi(n,\gamma)\chi'(n,\gamma)+6\zeta(3)+F(n,\gamma)-2\Phi(n,\gamma)-2\Phi(n,1-\gamma)\Big]\Big\}\langle\hat{\mathcal{U}}^Y(n,\gamma)\rangle\end{aligned}\tag{125}$$

where $\chi'(n,\gamma) \equiv \frac{d}{d\gamma}\chi(n,\gamma)$ etc.

Next we calculate the same thing using NLO BFKL results [3, 28]. The impact factor $\Phi_A(q)$ for the color dipole $\mathcal{U}(x,y)$ is proportional to $\alpha_s(q)(e^{iqx}-e^{iqy})(e^{-iqx}-e^{-iqy})$ so one obtains the cross section of the scattering of color dipole in the form

$$\langle\hat{\mathcal{U}}(x,0)\rangle \;=\; \frac{1}{4\pi^2}\int\frac{d^2q}{q^2}\frac{d^2q'}{q'^2}\alpha_s(q)(e^{iqx}-1)(e^{-iqx}-1)\Phi_B(q')\int_{a-i\infty}^{a+i\infty}\frac{d\omega}{2\pi i}\Big(\frac{s}{qq'}\Big)^{\omega}G_\omega(q,q') \tag{126}$$

where $G_\omega(q,q')$ is the partial wave of the forward reggeized gluon scattering amplitude satisfying the equation

$$\omega G_\omega(q,q') = \delta^{(2)}(q-q') + \int d^2pK(q,p)G_\omega(p,q') \tag{127}$$

and $\Phi_B(q')$ is the target impact factor. The kernel $K(q,p)$ is symmetric with respect to $q\leftrightarrow p$ and the eigenvalues are

$$\begin{aligned}\int d^2p\Big(\frac{p^2}{q^2}\Big)^{\gamma-1}e^{in\phi}K(q,p) \;&=\; \frac{\alpha_s(q)}{\pi}N_c\Big[\chi(n,\gamma)+\frac{\alpha_sN_c}{4\pi}\delta(n,\gamma)\Big], \qquad (128)\\ \delta(n,\gamma) \;&=\; -\frac{b}{2N_c}[\chi'(n,\gamma)+\chi^2(n,\gamma)]+\Big(\frac{67}{9}-\frac{\pi^2}{3}-\frac{10}{9}\frac{n_f}{N_c^3}\Big)\chi(n,\gamma)+6\zeta(3)\\ &\qquad -\chi''(n,\gamma)+F(n,\gamma)-2\Phi(n,\gamma)-2\Phi(n,1-\gamma)\Big\}\end{aligned}$$

The corresponding expression for $\langle\hat{\mathcal{U}}(n,\gamma)\rangle$ takes the form

$$\langle\hat{\mathcal{U}}(n,\gamma)\rangle \;=\; -\frac{1}{2\pi^2}\cos\frac{\pi n}{2}\frac{\Gamma(-\gamma+\frac{n}{2})}{\Gamma(1+\gamma+\frac{n}{2})}\int\frac{d^2q}{q^2}\frac{d^2q'}{q'^2}e^{-in\theta}\alpha_s(q)\Big(\frac{q^2}{4\mu^2}\Big)^{\gamma}\Phi_B(q')\int_{a-i\infty}^{a+i\infty}\frac{d\omega}{2\pi i}\Big(\frac{s}{qq'}\Big)^{\omega}G_\omega(q,q') \tag{129}$$

where θ is the angle between $\vec{q}$ and x axis. Using Eq. (127) we obtain

$$\begin{aligned}& s\frac{d}{ds}\langle\hat{\mathcal{U}}(n,\gamma)\rangle \qquad (130)\\ &= -\frac{1}{2\pi^2}\cos\frac{\pi n}{2}\frac{\Gamma(-\gamma+\frac{n}{2})}{\Gamma(1+\gamma+\frac{n}{2})}\int\frac{d^2q}{q^2}\frac{d^2q'}{q'^2}e^{-in\theta}\alpha_s(q)\Big(\frac{q^2}{4\mu^2}\Big)^{\gamma}\Phi_B(q')\int_{a-i\infty}^{a+i\infty}\frac{d\omega}{2\pi i}\Big(\frac{s}{qq'}\Big)^{\omega}\int d^2pK(q,p)G_\omega(p,q')\end{aligned}$$

The integration over q can be performed using

$$\int d^2q\;\alpha_s(q)\Big(\frac{q^2}{p^2}\Big)^{\gamma-1}e^{in\phi}K(q,p) \;=\; \frac{\alpha_s^2(p)}{\pi}N_c\Big[\chi(n,\gamma)-\frac{b\alpha_s}{4\pi}\chi'(n,\gamma)+\frac{\alpha_sN_c}{4\pi}\delta(n,\gamma)\Big] \tag{131}$$

(recall that $K(q,p)=K(p,q)$ and $\alpha_s(p)=\alpha_s-\frac{b\alpha_s^2}{4\pi}\ln\frac{p^2}{\mu^2}$ with our accuracy). The result is

$$\begin{aligned}s\frac{d}{ds}\langle\hat{\mathcal{U}}(n,\gamma)\rangle \;&=\; -\frac{\alpha_s}{2\pi^2}\cos\frac{\pi n}{2}\frac{\Gamma(-\gamma+\frac{n}{2})}{\Gamma(1+\gamma+\frac{n}{2})}\int\frac{d^2p}{p^2}\frac{d^2q'}{q'^2}e^{-in\varphi}\Big(\frac{p^2}{4\mu^2}\Big)^{\gamma}\Phi_B(q') \qquad (132)\\ \times&\int_{a-i\infty}^{a+i\infty}\frac{d\omega}{2\pi i}\Big(\frac{s}{pq'}\Big)^{\omega}G_\omega(p,q')\frac{\alpha_s(p)}{\pi}N_c\Big[\chi(n,\gamma-\frac{\omega}{2})-\frac{b\alpha_s}{4\pi}\chi'(n,\gamma-\frac{\omega}{2})+\frac{\alpha_sN_c}{4\pi}\delta(n,\gamma-\frac{\omega}{2}))\Big]\end{aligned}$$

where the angle φ corresponds to $\vec{p}$. Since $\omega\sim\alpha_s$ we can neglect terms $\sim\omega$ in the argument of δ and expand $\chi(n,\gamma-\frac{\omega}{2})\simeq\chi(n,\gamma)-\frac{\omega}{2}\chi'(n,\gamma)$. Using again Eq. (127) in the leading order we can replace extra ω by $\frac{\alpha_s}{\pi}N_c\chi(n,\gamma)$ and obtain

$$\begin{aligned}s\frac{d}{ds}\langle\hat{\mathcal{U}}(n,\gamma)\rangle \;&=\; -\frac{\alpha_s}{2\pi^2}\cos\frac{\pi n}{2}\frac{\Gamma(-\gamma+\frac{n}{2})}{\Gamma(1+\gamma+\frac{n}{2})}\int\frac{d^2p}{p^2}\frac{d^2q'}{q'^2}e^{-in\varphi}\Big(\frac{p^2}{4\mu^2}\Big)^{\gamma}\\ \times\;\Phi_B(q')&\int_{a-i\infty}^{a+i\infty}\frac{d\omega}{2\pi i}\Big(\frac{s}{pq'}\Big)^{\omega}G_\omega(p,q')\frac{\alpha_s^2(p)}{\pi}N_c\Big[\chi(n,\gamma)-\frac{b\alpha_s}{4\pi}\chi'(n,\gamma)+\frac{\alpha_sN_c}{4\pi}[\delta(n,\gamma)-2\chi(n,\gamma)\chi'(n,\gamma)]\Big] \qquad (133)\end{aligned}$$

Finally, expanding $\alpha_s^2(p)\simeq\alpha_s(p)(\alpha_s-\frac{b\alpha_s^2}{4\pi}\ln\frac{p^2}{\mu^2})\alpha_s(\mu)$ we obtain

$$s\frac{d}{ds}\langle\hat{\mathcal{U}}(n,\gamma)\rangle \;=\; -\frac{\alpha_sN_c}{2\pi^3}\cos\frac{\pi n}{2}\frac{\Gamma(-\gamma+\frac{n}{2})}{\Gamma(1+\gamma+\frac{n}{2})}\Big\{\chi(n,\gamma)\Big(1-\frac{b\alpha_s}{4\pi}\frac{d}{d\gamma}-\ln 4+2C\Big)-\frac{b\alpha_s}{4\pi}\chi'(n,\gamma)$$
$$+\;\frac{\alpha_sN_c}{4\pi}[\delta(n,\gamma)-2\chi(n,\gamma)\chi'(n,\gamma)]\Big\}\int\frac{d^2p}{p^2}\frac{d^2q'}{q'^2}e^{-in\varphi}\alpha_s(p)\Big(\frac{p^2}{4\mu^2}\Big)^{\gamma}\Phi_B(q')\int_{a-i\infty}^{a+i\infty}\frac{d\omega}{2\pi i}\Big(\frac{s}{pq'}\Big)^{\omega}G_\omega(p,q') \quad (134)$$

which can be rewritten as an evolution equation

$$s\frac{d}{ds}\langle\hat{\mathcal{U}}(n,\gamma)\rangle$$
$$=\;\frac{\alpha_sN_c}{\pi}\Big\{\Big(1+\frac{b\alpha_s}{4\pi}\Big[\chi(n,\gamma)-\frac{2\gamma}{\gamma^2-\frac{n^2}{4}}+2C-\ln 4-\frac{d}{d\gamma}\Big]\Big)\chi(n,\gamma)+\frac{\alpha_sN_c}{4\pi}[\delta(n,\gamma)-2\chi(n,\gamma)\chi'(n,\gamma)]\Big\}\langle\mathcal{U}(n,\gamma)\rangle$$
$$=\;\frac{\alpha_sN_c}{\pi}\Big\{\Big[1+\frac{b\alpha_s}{4\pi}\big(2C-\ln 4-\frac{d}{d\gamma}\big)+\frac{\alpha_sN_c}{4\pi}\Big(\frac{67}{9}-\frac{\pi^2}{3}-\frac{10}{9}\frac{n_f}{N_c^3}\Big)\Big]\chi(n,\gamma)+\frac{\alpha_sb}{8\pi}\Big[\chi^2(n,\gamma)-\chi'(n,\gamma)-\frac{4\gamma\chi(\gamma)}{\gamma^2-\frac{n^2}{4}}\Big]$$
$$+\;\frac{\alpha_sN_c}{4\pi}\Big[-\chi''(n,\gamma)-2\chi(n,\gamma)\chi'(n,\gamma)+6\zeta(3)+F(n,\gamma)-2\Phi(n,\gamma)-2\Phi(n,1-\gamma)\Big]\Big\}\langle\hat{\mathcal{U}}(n,\gamma)\rangle \quad (135)$$

We see that this eigenvalue coincides with Eq. (125).

---

[1] L.N. Lipatov, *Sov.J.Nucl.Phys.***23**338(1976)

[2] V.S. Fadin, E.A. Kuraev, and L.N. Lipatov, *Sov.Phys.JETP* **44**:443-450,1976, *Sov.Phys.JETP* **45**,199 (1977); I. Balitsky and L.N. Lipatov, *Sov. Journ. Nucl. Phys.* **28**, 822 (1978).

[3] V.S. Fadin and L.N. Lipatov, *Phys. Lett.* **B429**, 127 (1998).

[4] G. Camici and M. Ciafaloni, *Phys. Lett.* **B430**, 349 (1998).

[5] A. Vogt, S. Moch, and J.A.M. Vermaseren, *Nucl.Phys.* **B691**, 129 (2004)

[6] J. Bartels and A. Kyrieleis, *Phys. Rev.* **D70**,114003(2004); J. Bartels, D. Colferai, S. Gieseke, and A. Kyrieleis, *Phys. Rev.* **D66**, 094017 (2002). J. Bartels, S. Gieseke, and A. Kyrieleis, *Phys. Rev.* **D65**, 014006 (2002).

[7] I. Balitsky, *Nucl. Phys.* **B463**, 99 (1996); *"Operator expansion for diffractive high-energy scattering"*, [hep-ph/9706411];

[8] I. Balitsky, *"High-Energy QCD and Wilson Lines"*, In *Shifman, M. (ed.): At the frontier of particle physics, vol. 2*, p. 1237-1342 (World Scientific, Singapore,2001) [hep-ph/0101042]

[9] A.H. Mueller, *Nucl. Phys.* **B415**, 373 (1994); A.H. Mueller and Bimal Patel, *Nucl. Phys.* **B425**, 471 (1994).

[10] N.N. Nikolaev and B.G. Zakharov, *Phys. Lett.* **B 332**, 184 (1994); *Z. Phys.* **C64**, 631 (1994); N.N. Nikolaev B.G. Zakharov, and V.R. Zoller, *JETP Letters* **59**, 6 (1994).

[11] Yu.V. Kovchegov, *Phys. Rev.* **D60**, 034008 (1999); *Phys. Rev.* **D61**,074018 (2000).

[12] L.V. Gribov, E.M. Levin, and M.G. Ryskin, *Phys. Rept.* **100**, 1 (1983), A.H. Mueller and J.W. Qiu, *Nucl. Phys.* **B268**, 427 (1986); A.H. Mueller, *Nucl. Phys.* **B335**, 115 (1990).

[13] E. Iancu and R. Venugopalan , In *Hwa, R.C. (ed.) et al.: Quark gluon plasma* 249-3363, [e-Print: hep-ph/0303204];
H. Weigert , *Prog.Part.Nucl.Phys.* **55**, 461(2005);
J. Jalilian-Marian and Yu.V. Kovchegov, *Prog.Part.Nucl.Phys.* **56**, 104(2006).

[14] I. Balitsky and G.A. Chirilli, *Nucl. Phys.***B822**, 45 (2009).

[15] L.N. Lipatov, *Sov. Phys. JETP* **63**, 904 (1986).

[16] J.M. Maldacena, *Phys.Rev.Lett.* **80**, 4859 (1998).

[17] I. Balitsky and A.V. Belitsky, *Nucl. Phys.* **B629**, 290 (2002).

[18] I. Balitsky, *Phys.Rev.* **D75**, 014001 (2007).

[19] I. Balitsky and G.A. Chirilli, *Phys.Rev.* **D77**, 014019(2008)

[20] I. Balitsky, *Phys. Lett.* **B 124**, 230 (1983);

[21] I. Balitsky and V.M. Braun, *Nucl. Phys.* **B311**, 541 (1989).

[22] I. Balitsky and V.M. Braun, *Nucl. Phys.* **B361**, 93 (1991).

[23] A.H. Mueller and H. Navelet, *Nucl. Phys.* **B282**, 727 (1987).

[24] A.V. Belitsky, S.E. Derkachov, G.P. Korchemsky, and A.N. Manashov, *Phys.Rev.* **D70**, 045021 (2004).

[25] L. Cornalba, *Eikonal methods in AdS/CFT: Regge theory and multi-reggeon exchange*, arXiv:0710.5480 [hep-th];

[26] L. Cornalba, M.S. Costa, and J. Penedones, *JHEP* **048**, 0806 (2008);

[27] I. Balitsky and G.A. Chirilli, *Phys.Rev.* **D79**, 031502 (2009)

[28] A.V. Kotikov and L.N. Lipatov, *Nucl. Phys.* **B582**, 19 (2000); *Nucl. Phys.* **B5661**, 19 (2003). Erratum-ibid., **B685**, 405 (2004).

[29] A.V. Kotikov, L.N. Lipatov, A.I. Onishchenko, and V.N. Velizhanin, *Phys.Lett.* **B595**, 521 (2004); Erratum-ibid.**B632**,754 (2006).

[30] R.C. Brower, J. Polchinski, M. J. Strassler, Chung-I Tan, *JHEP* **005**, 0712 (2007)

[31] L. Cornalba, M.S. Costa, and J. Penedones, *Deep Inelastic Scattering in Conformal QCD*, arXiv:0911.0043 [hep-th]
[32] J. Penedones, *High Energy Scattering in the AdS/CFT Correspondence*, arXiv:0712.0802 [hep-th]
[33] I. Balitsky, *Phys. Rev.* **D60**, 014020 (1999).
[34] E. D'Hoker, D.Z. Freedman, and W. Skiba, *Phys. Rev.* **D59**, 045008(1999)
[35] V.S. Fadin, R. Fiore, A.V. Grabovsky, *Nucl. Phys.* **B831**, 248 (2010); V.S. Fadin, R. Fiore, *Phys. Lett.* **B661**, 139 (2008).
[36] I. Balitsky and G.A. Chirilli, arXiv:0911.5192 [hep-ph]
[37] M. Beneke, *Phys.Rept.* **317**,1(1999); M. Beneke and V.M. Braun, *"Renormalons and power corrections."*, In *Shifman, M. (ed.): At the frontier of particle physics, vol. 3*, p. 1719-1773 (World Scientific, Singapore,2001) [hep-ph/0010208]
[38] Yu. V. Kovchegov and H. Weigert, *Nucl. Phys.* **A784**, 188 (2007),
[39] J. L. Albacete, Yu. V. Kovchegov, *Phys. Rev.* **D75**, 125021(2007).
[40] J. Bartels, A. Sabio Vera, and F. Schwennsen *JHEP* 0611:051(2006).
[41] F. Caporale, D. Yu. Ivanov and A. Papa, *Eur. Phys. J* **C58**, 1 (2008).
[42] Yu. V. Kovchegov and H. Weigert, *Nucl.Phys.* **A789**, 260(2007).
[43] In principle, there may be a pure gauge field outside the shock wave. This does not change our result for the coefficient function in front of color dipole operator, see the discussion in Ref. [7, 8]